

BICEP/Keck: Constraining primordial gravitational waves with CMB polarization observations from the South Pole



Marion Dierickx for the BICEP/Keck Collaboration – APC, June 1st 2018



Photo credit: R. Schwarz

I. Inflation and the CMB

II. The BICEP/Keck
experiment

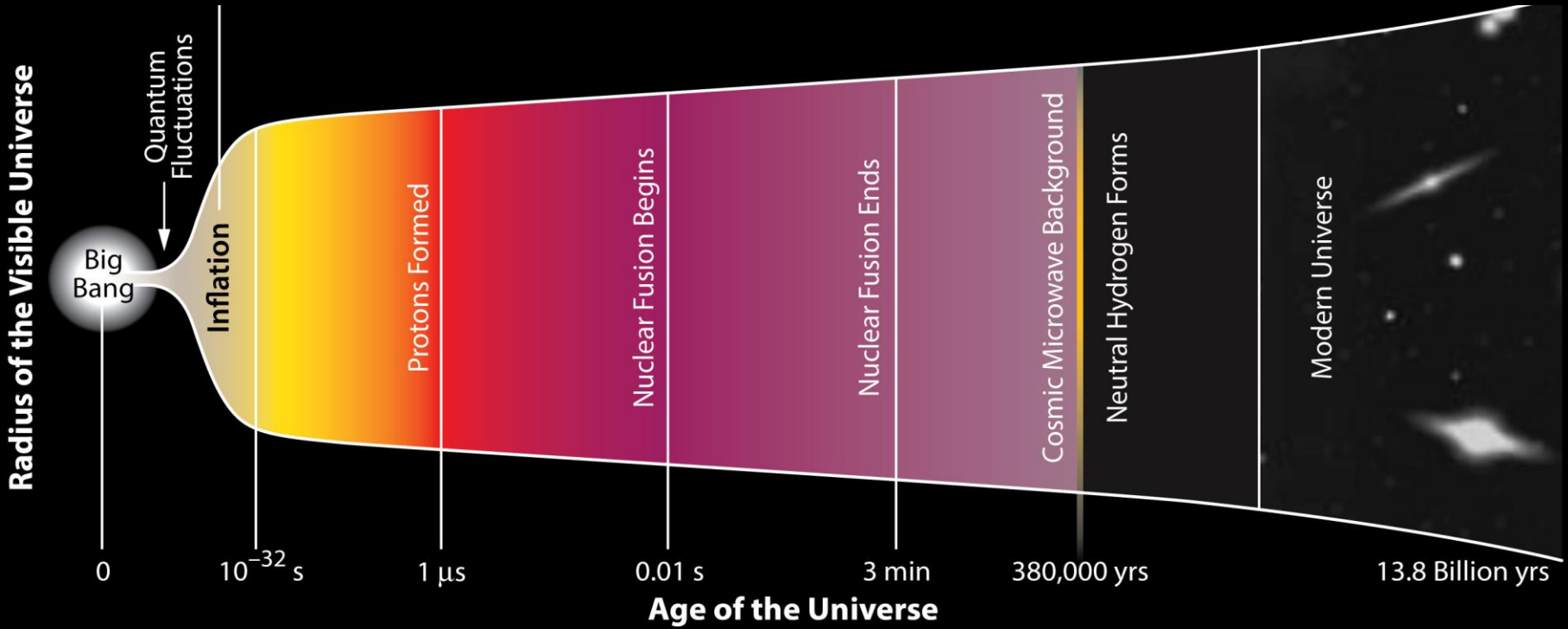
III. BK14, 15: Results
with data up to 2015

IV. What's next?
BICEP3 and BICEP Array

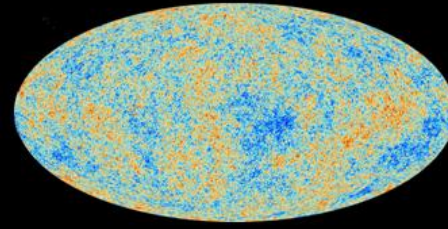
I.

Inflation and the CMB

History of the Universe



Photon decoupling



Earliest Time
Visible with Light

Neutral Hydrogen Forms

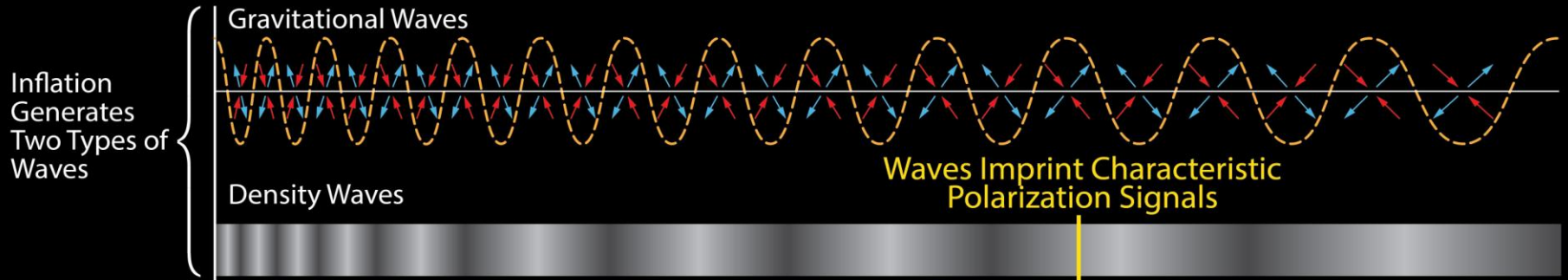
Modern Universe

380,000 yrs

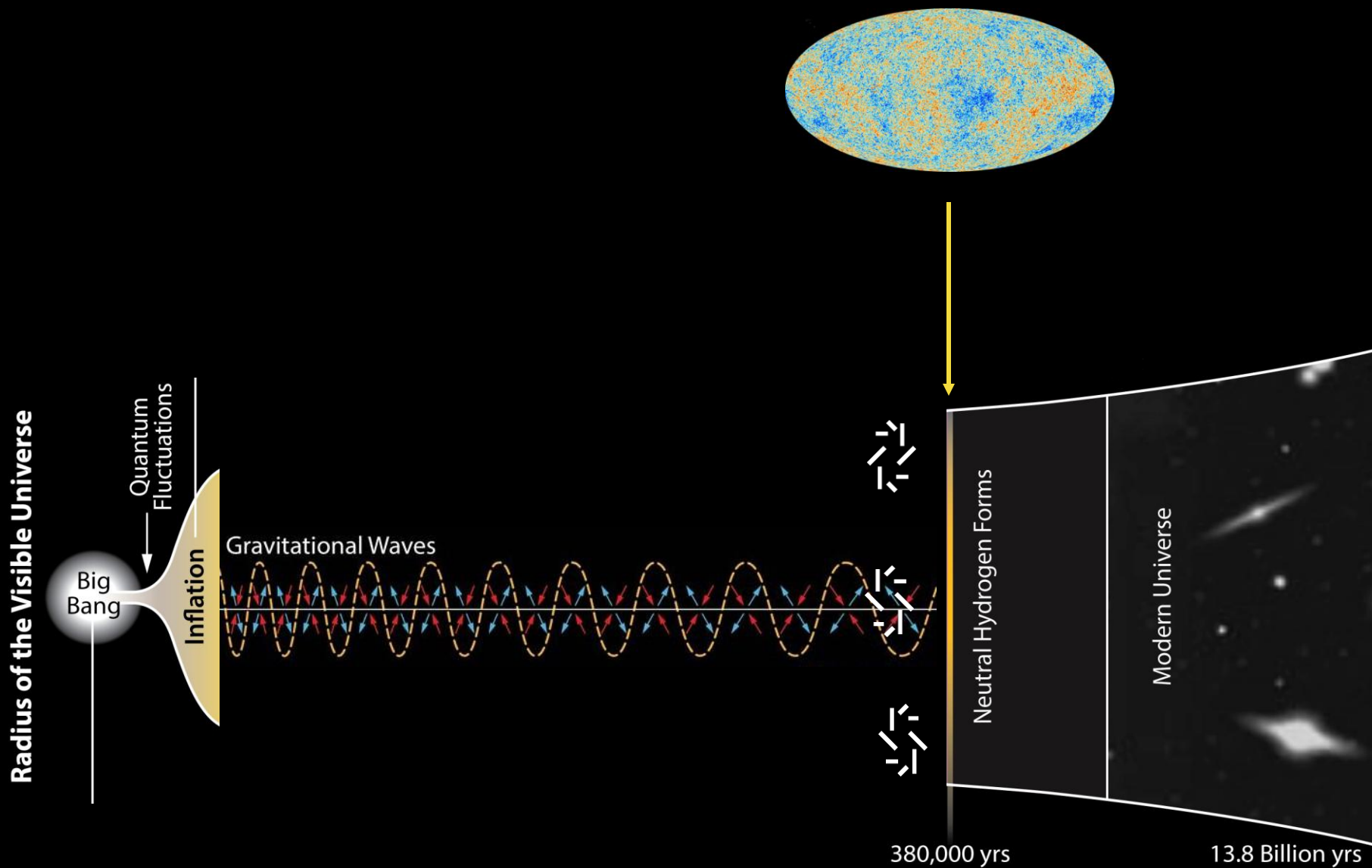
13.8 Billion yrs



Inflation

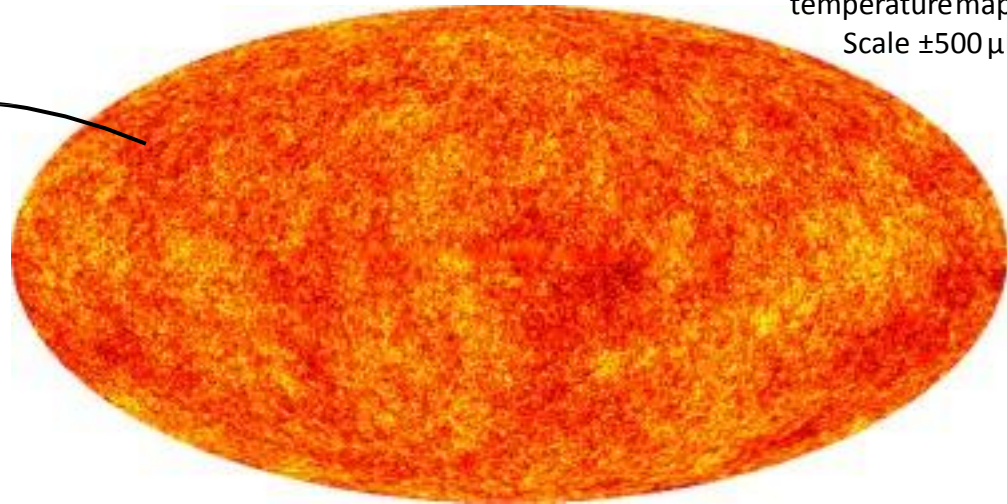
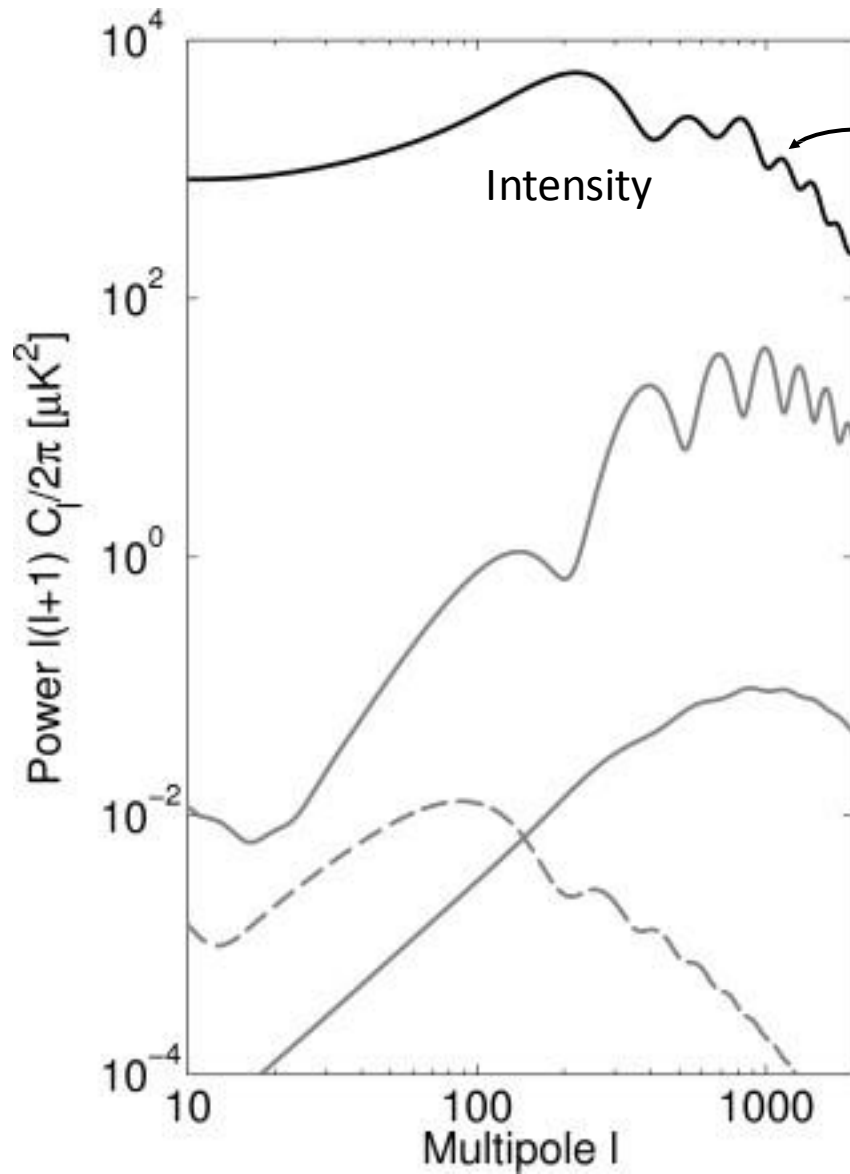


Imprint on the CMB

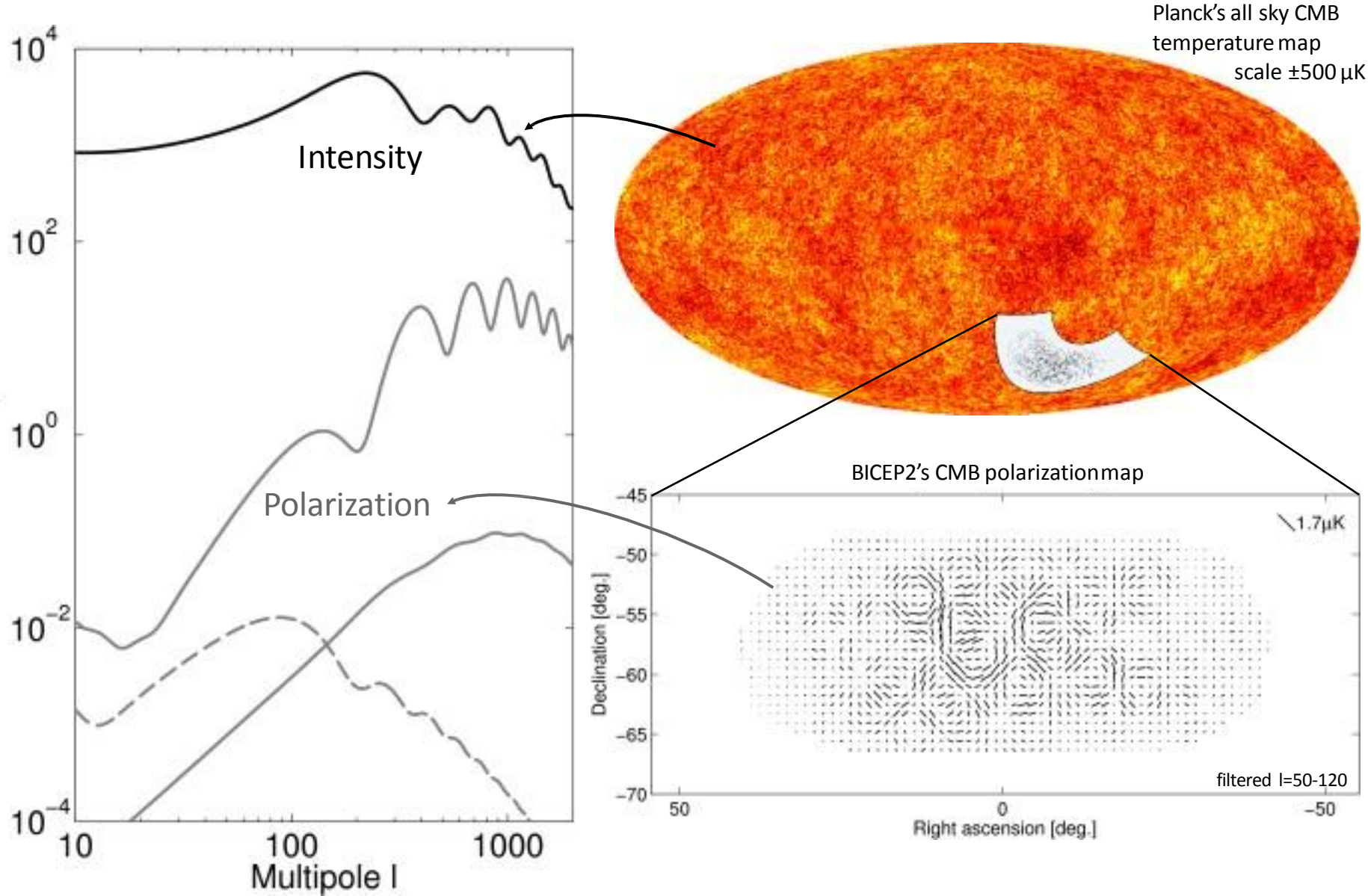


Cosmic Microwave Background

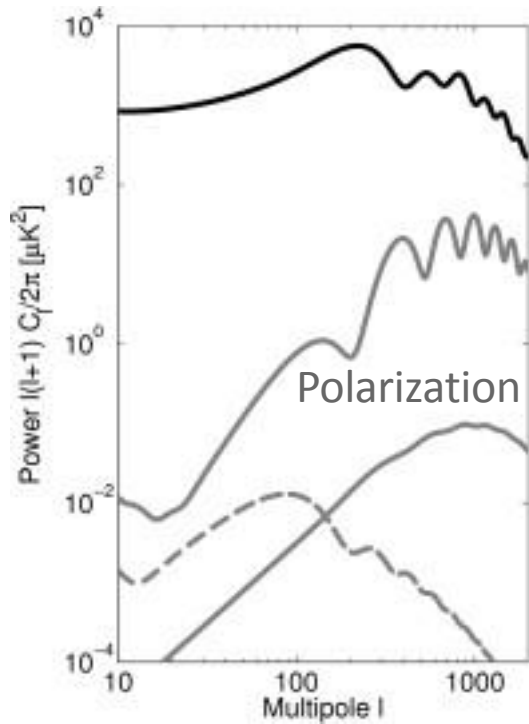
Planck's all sky CMB
temperature map.
Scale $\pm 500 \mu\text{K}$



Cosmic Microwave Background

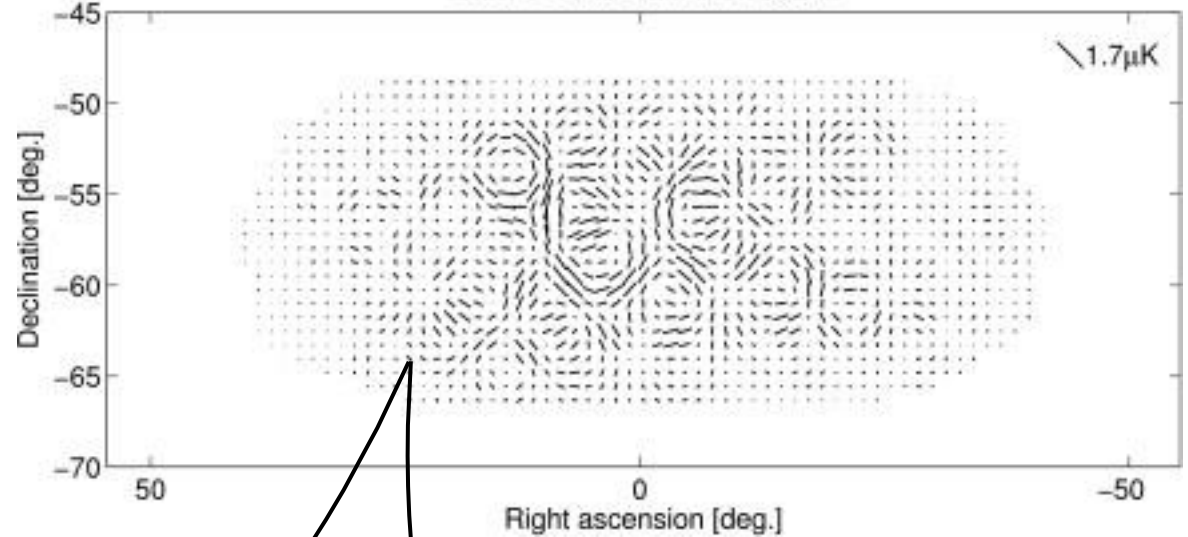


CMB Polarization

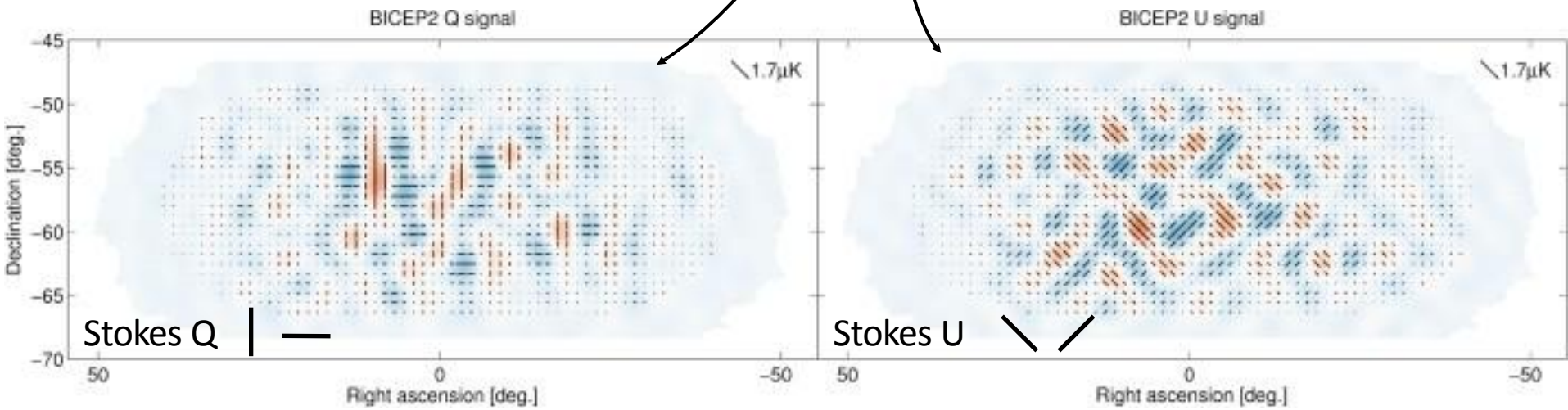


Need 2D basis to describe polarization map...

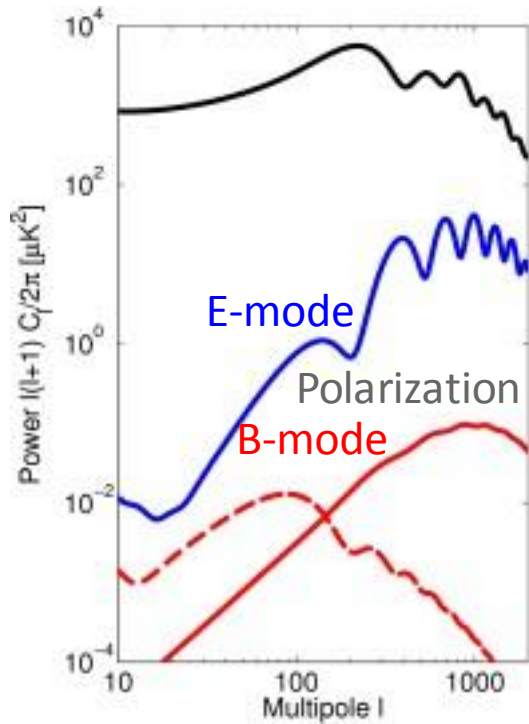
BICEP2's CMB polarization map



... familiar choice: Stokes Parameters Q&U

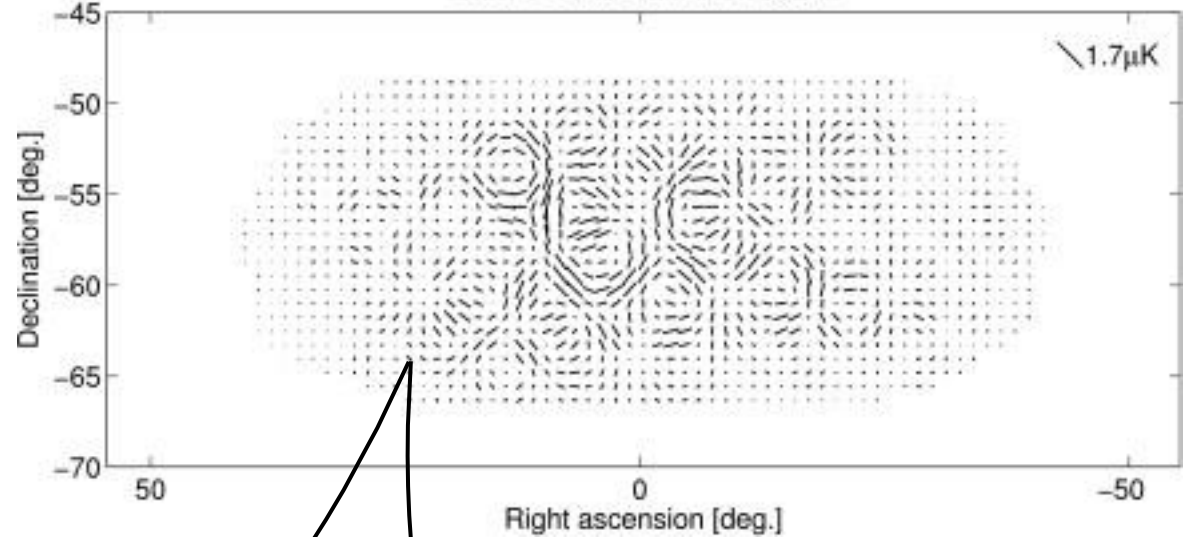


CMB Polarization

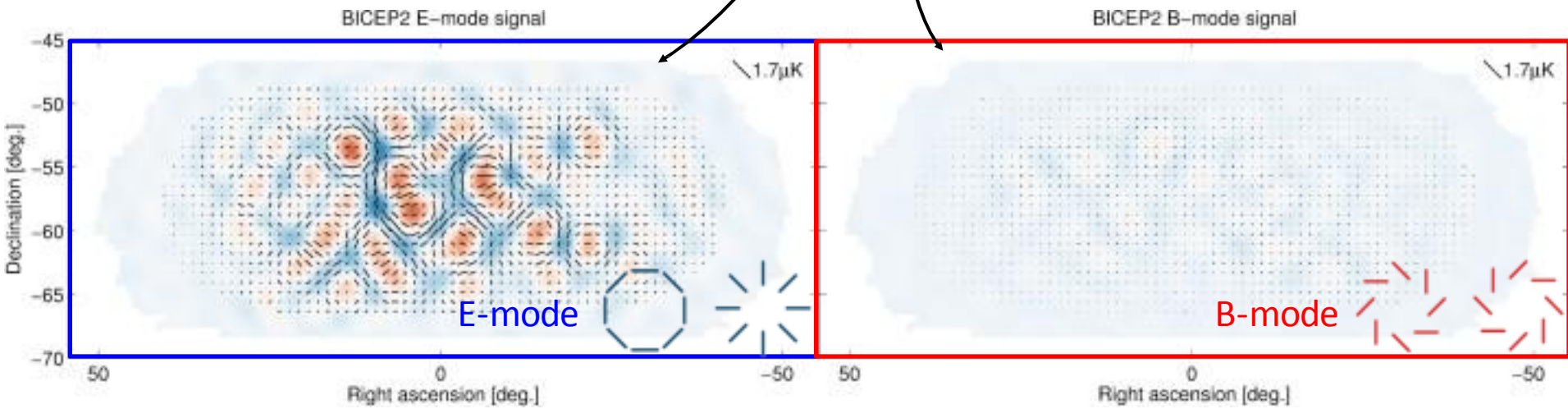


Need 2D basis to describe polarization map...

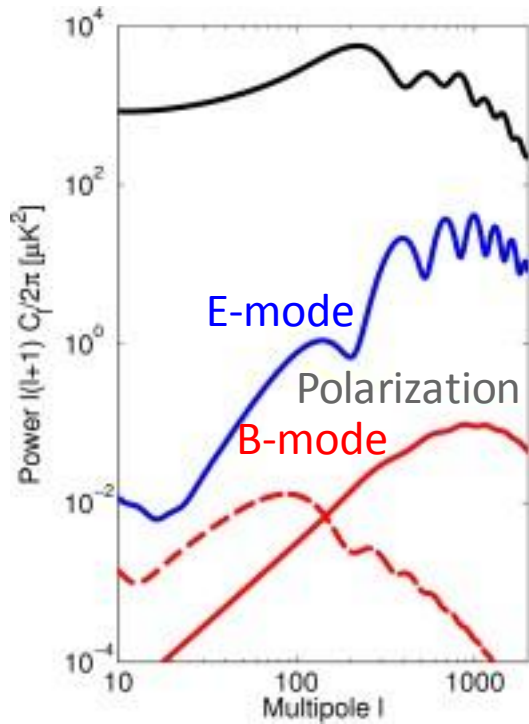
BICEP2's CMB polarization map



... clever choice for cosmology: E&B-modes

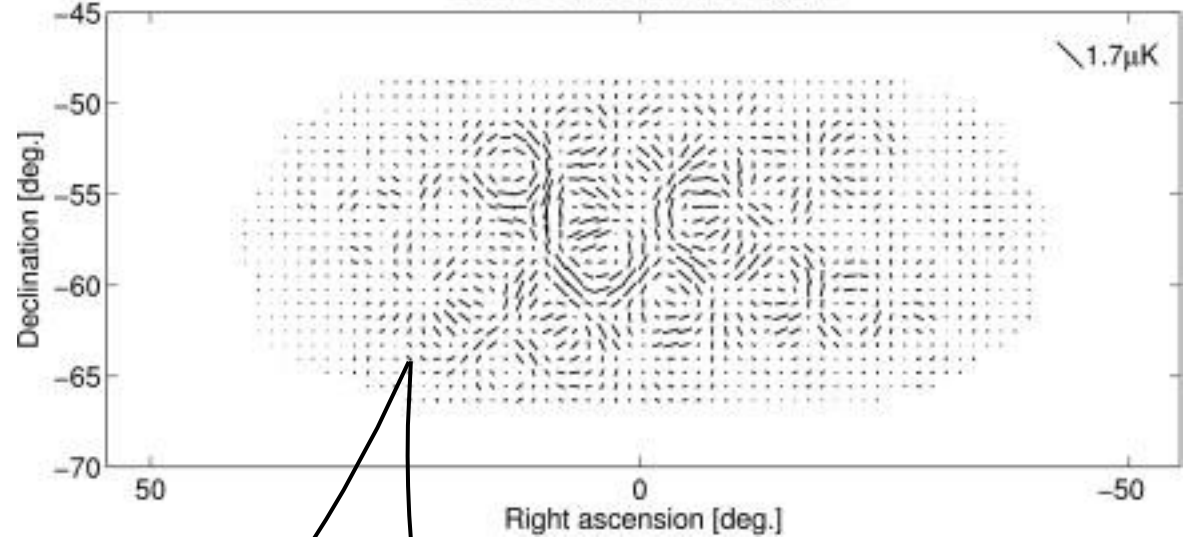


CMB Polarization

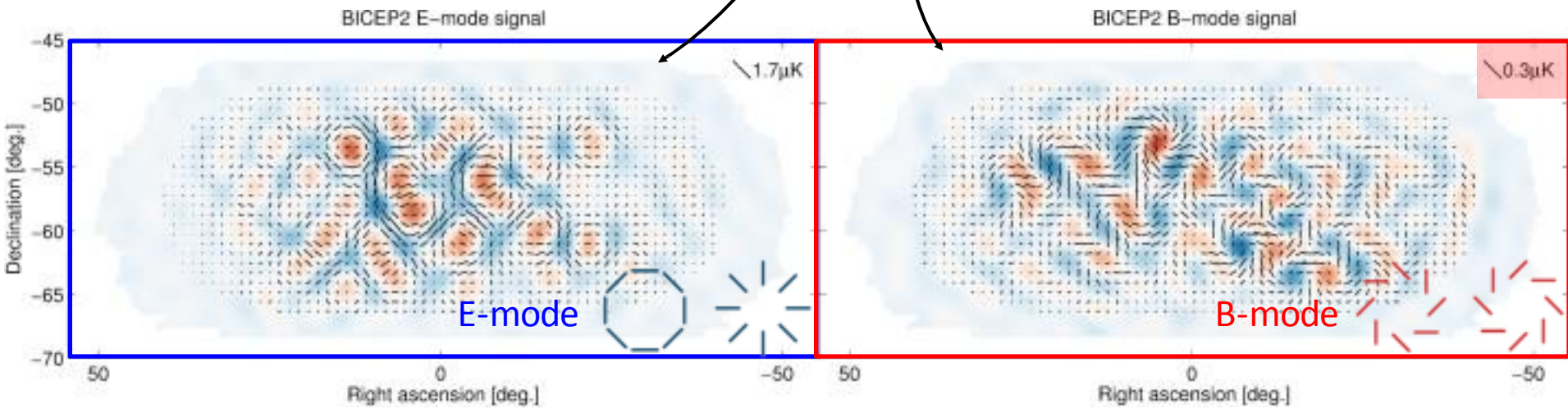


Need 2D basis to describe polarization map...

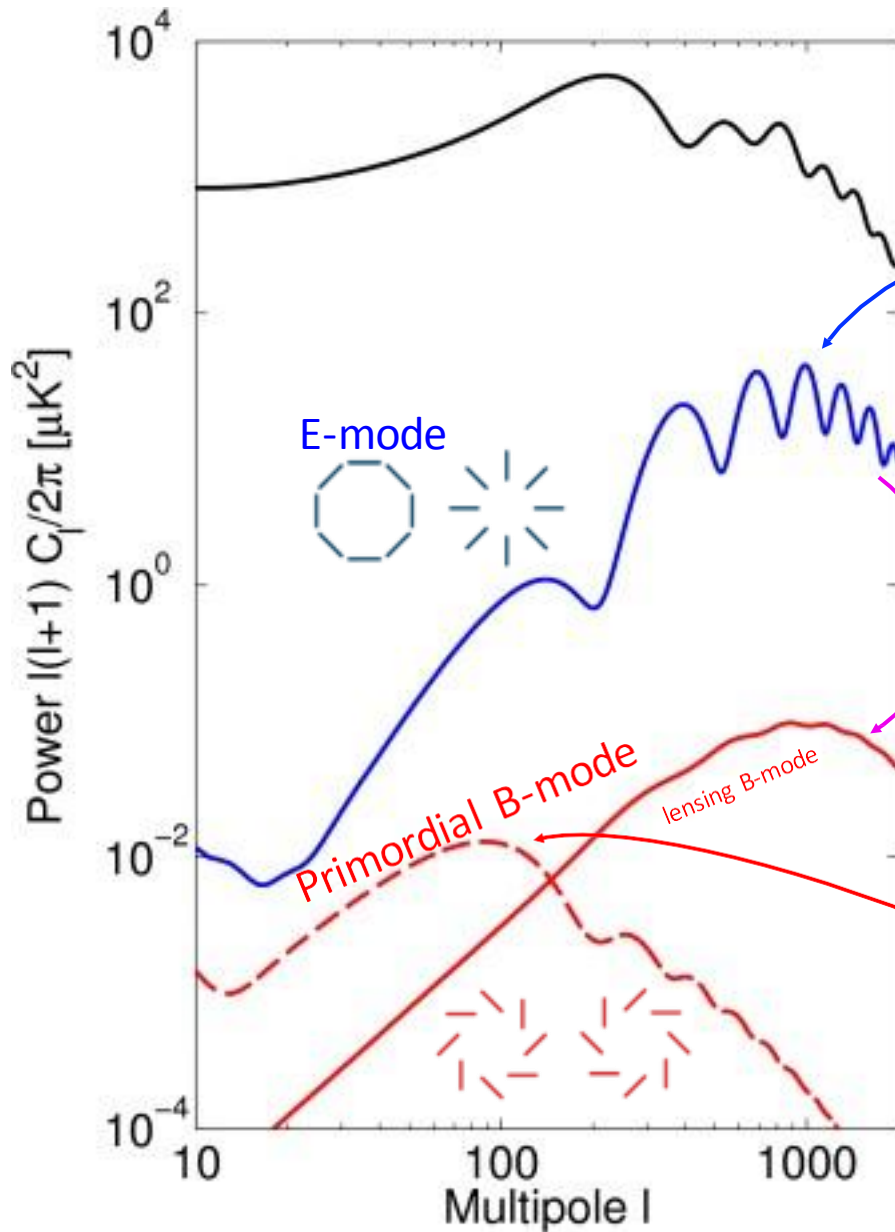
Bicep2's CMB polarization map



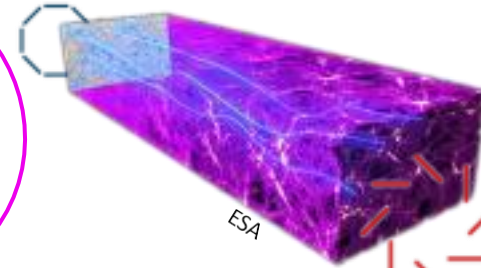
... clever choice for cosmology: E&B-modes



CMB Polarization



In standard Λ CDM only E-modes are present at last scattering



During propagation some of the E-modes are confused into B-modes by lensing

Inflationary gravitational waves are unique source of B-modes
→ peaking at $l \approx 100$: degreescales

II.

The BICEP/Keck Experiment



UNIVERSITY OF TORONTO



The South Pole



The South Pole



Why there?

- High altitude (9,300 ft = 2,800 m, most of it ice)
- Lack of day/night cycles makes for a very stable atmosphere
- Consistently dry
- Southern Hole observable for 6 months of continuous darkness
- Minimal radio frequency interference





... ..



The Dark Sector



BICEP1
BICEP2
BICEP3



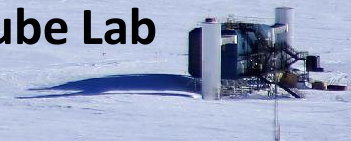
DASI
QUAD
Keck Array
BICEP Array



South Pole Telescope
(SPT-3G)



IceCube Lab



The Dark Sector



BICEP/Keck Experimental Strategy:

- Target 2-degree peak of B-mode power spectrum
- Relentless observation of the same 1% patch of sky since 2006
- Small-aperture refractive optics (cheap, low systematics)
- Initial effort at 150 GHz, now multi-frequency observations

BICEP1
BICEP2
BICEP3



South Pole Telescope
(SPT-3G)

DASI
QUAD
Keck Array
BICEP Array



IceCube Lab





BICEP2

x 5 =



Keck Array

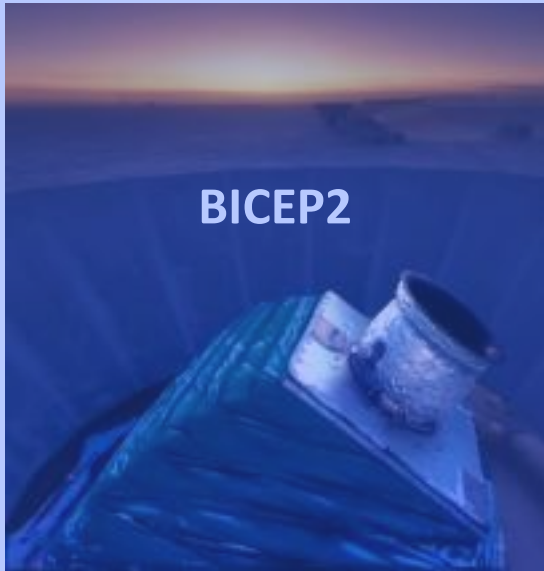


BICEP3

x 4 =



BICEP Array



BICEP2

x 5 =



Keck Array



BICEP3

x 4 =



BICEP Array



x 5 =



x 4 =



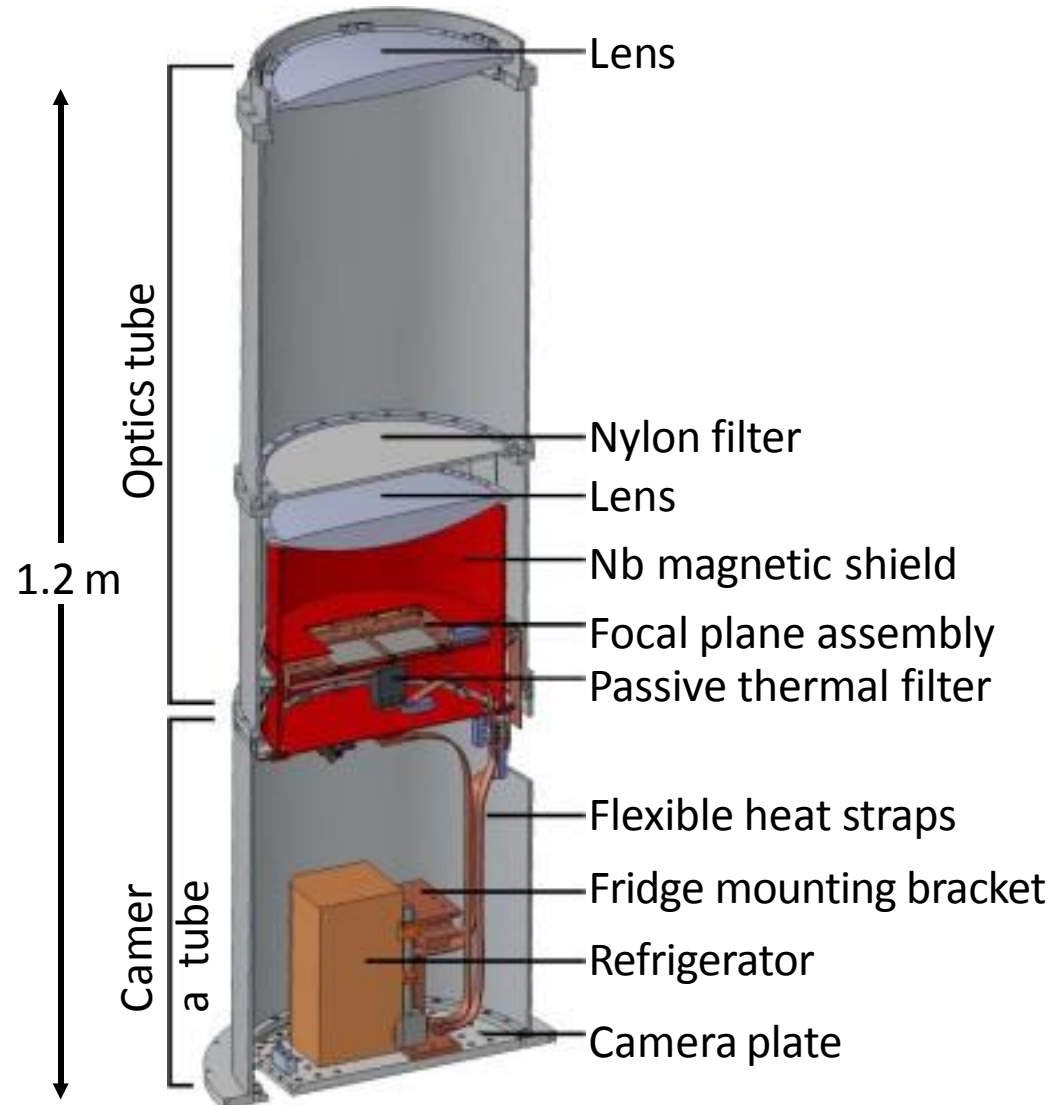
The BICEP2/Keck Telescopes

Telescope as compact as possible while allowing angular resolution to observe degree-scale features.

On-axis, refractive optics allow the entire telescope to rotate around boresight for polarization modulation.

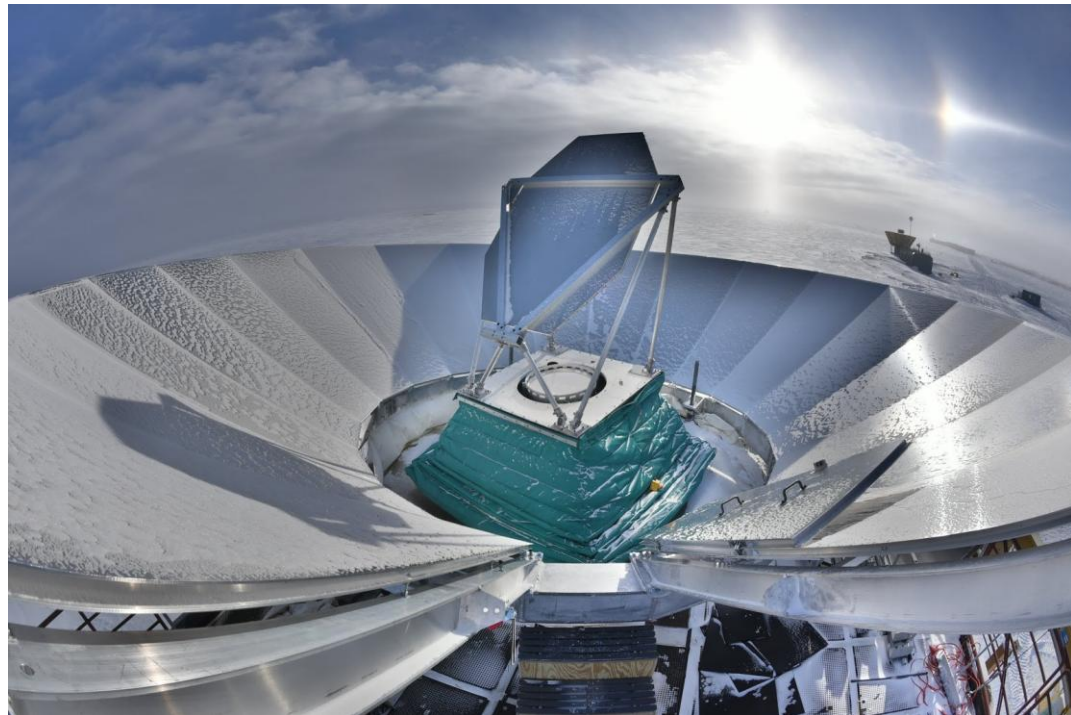
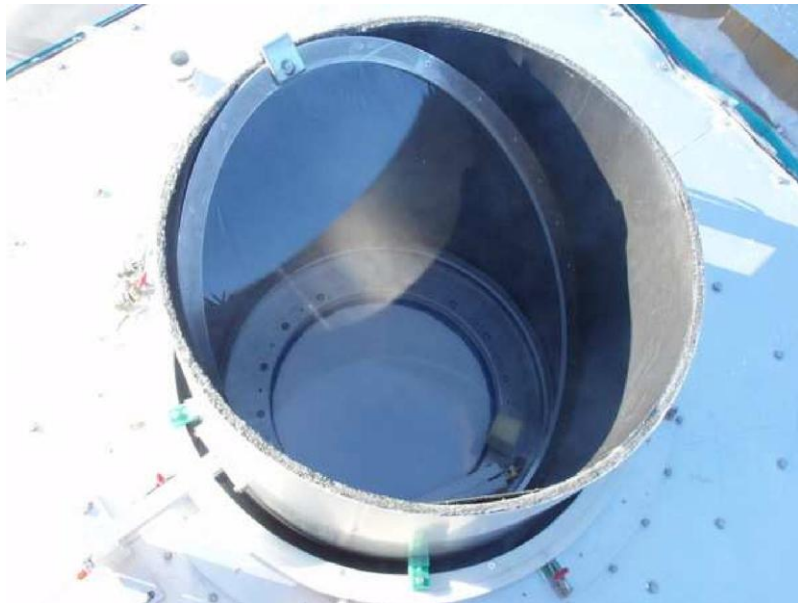
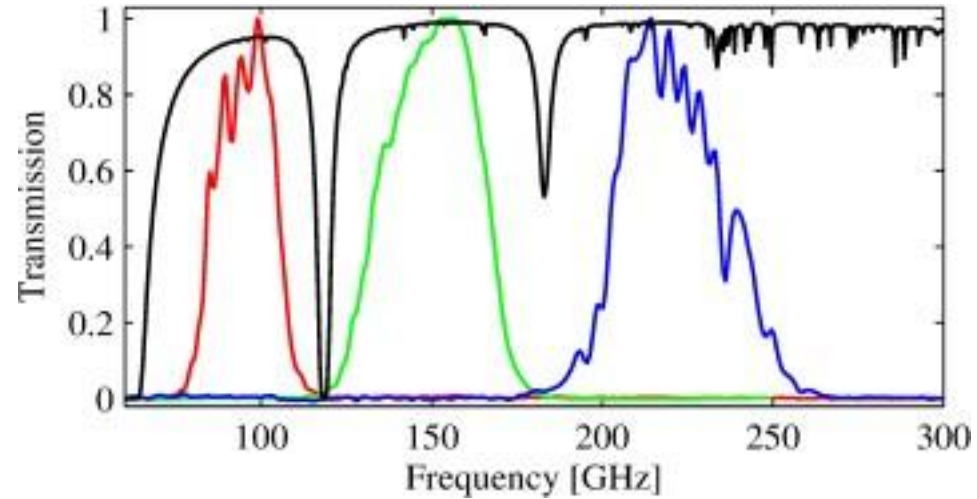
Pulse tube cryogenic cooler cools the optical elements to 4.2 K.

A 3-stage helium sorption refrigerator further cools the detectors to 0.27 K.



BICEP/Keck Calibrations

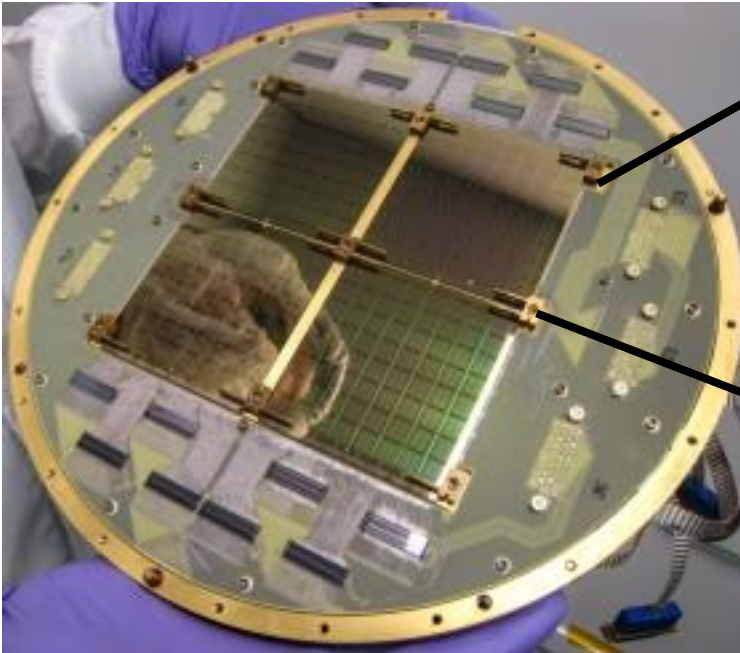
- Optical Efficiency
- Near-field Beam Mapping
- FTS
- Thick grill filter
- Forebaffle Loading
- Far sidelobe mapping
- Far-field beam mapping
- Polarization calibration
 - Rotating Polarized Source
 - Dielectric Sheet Calibrator



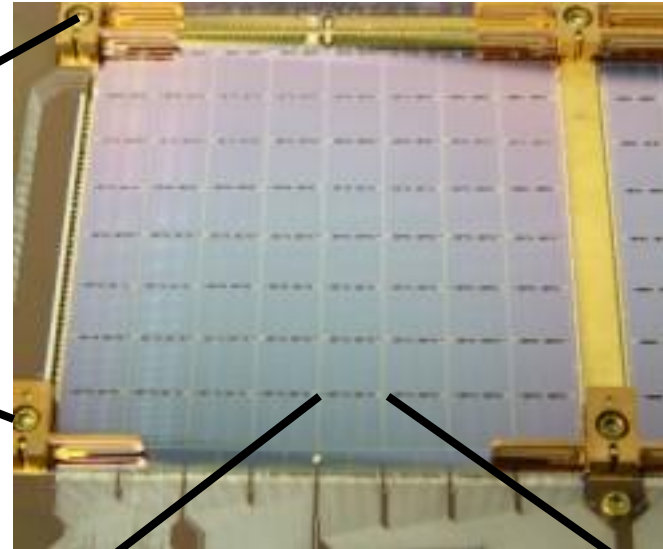
Detector Technology



Focal Plane



Planar Antenna Array



One pixel



Microstrip filters

Slot antennas

Transition Edge Sensor



BICEP2/Keck Band Response

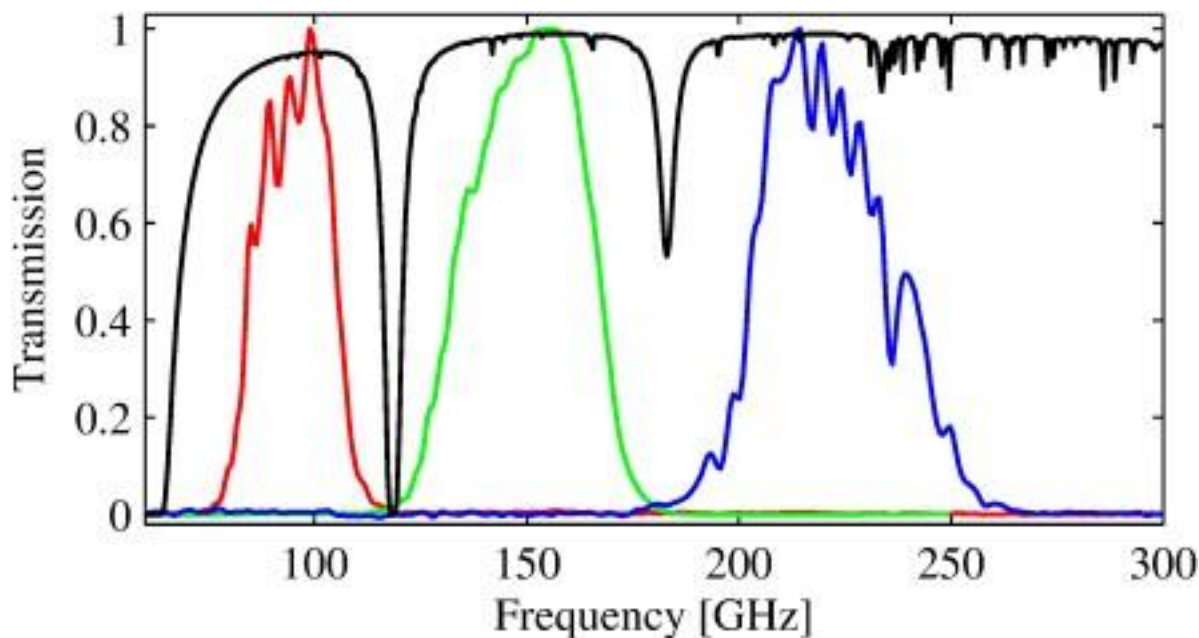


The detector passbands are defined by a filter printed directly onto the focal plane wafers.

The ~25% fractional bandwidth fits within atmospheric transmission windows straddled by oxygen and water lines.

In these windows, the atmosphere is transparent to microwaves.

Typical South Pole atmospheric transmission



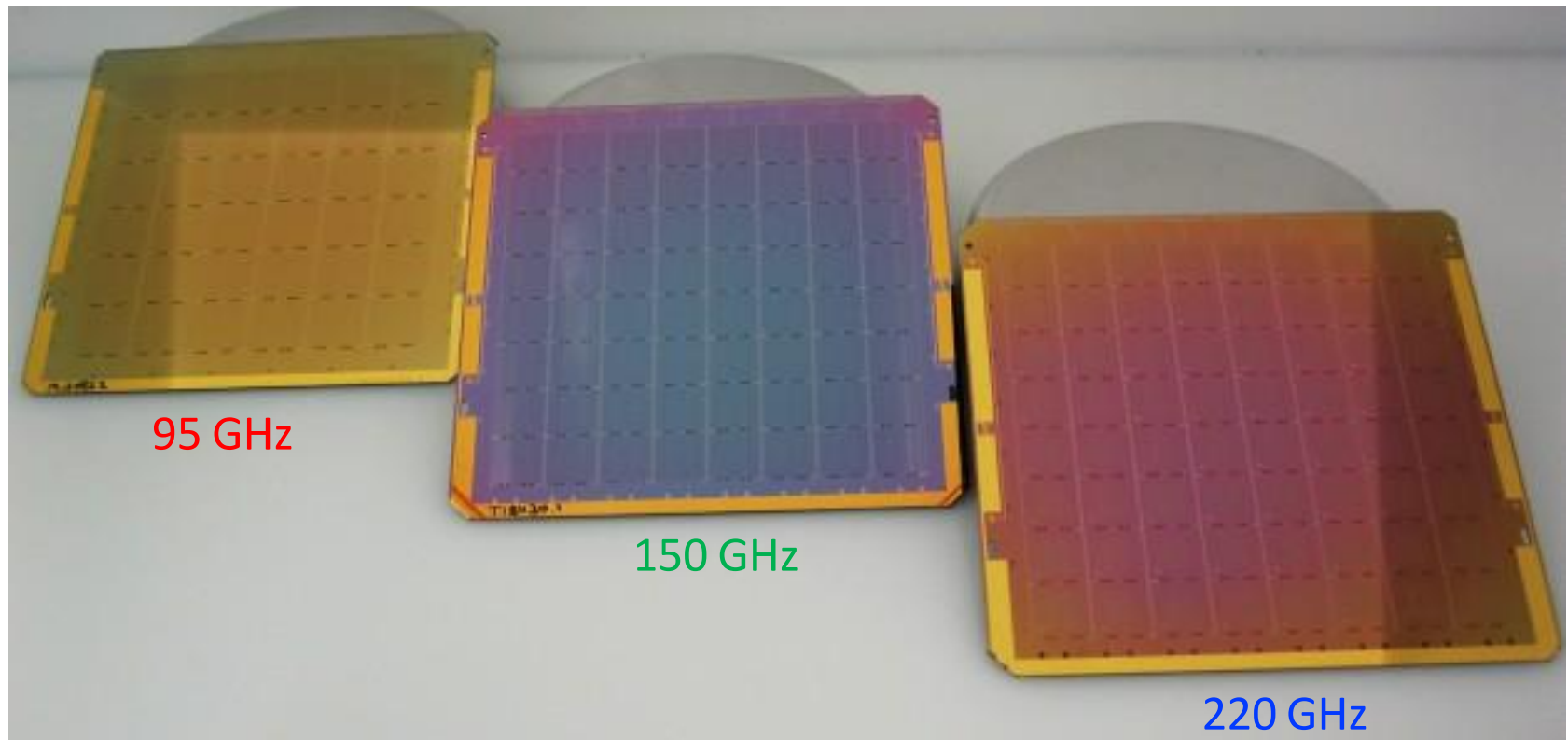
Choices of instrument response:

95 GHz

150 GHz

220 GHz

Detectors designed to scale in frequency



Up to 2013 – all 150 GHz

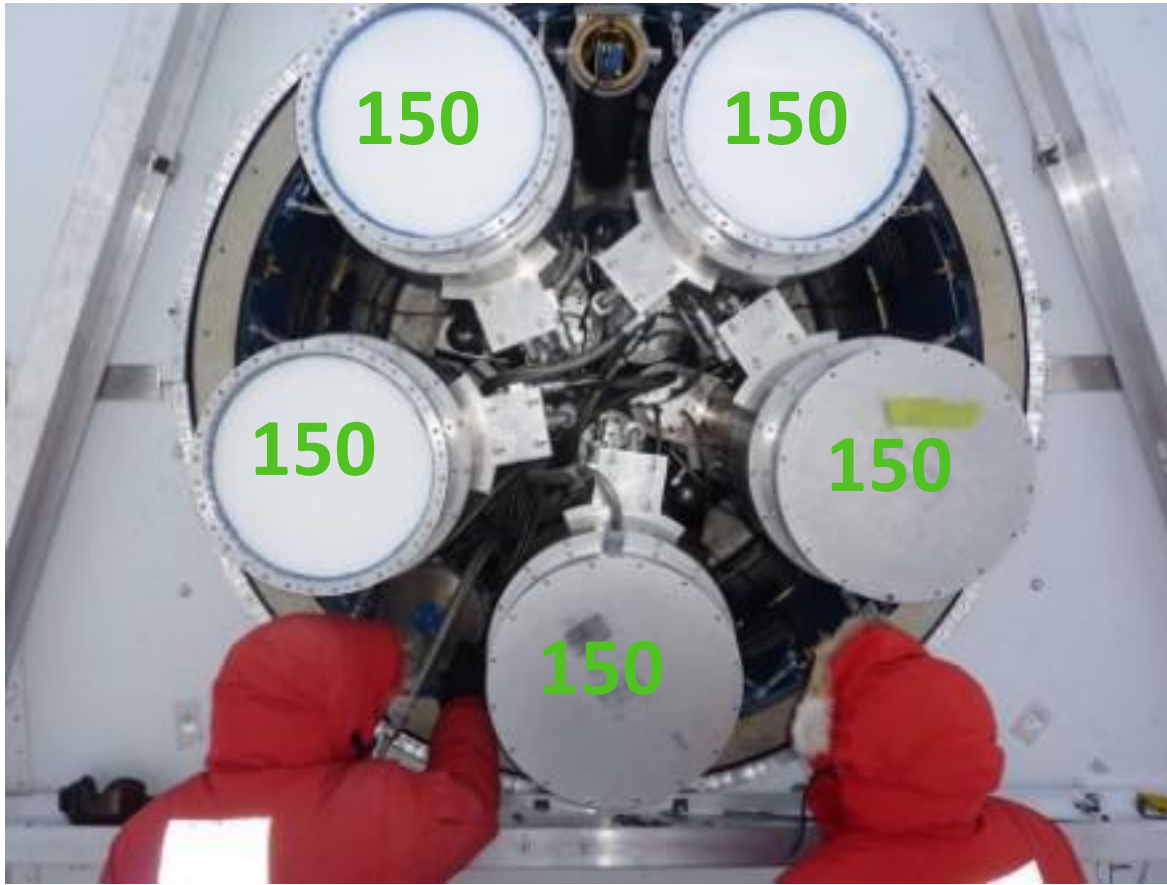
2014 – 95/150 GHz

2015 – 95/150/220 GHz

2017 – 220/270 GHz

Keck Array Frequency Coverage

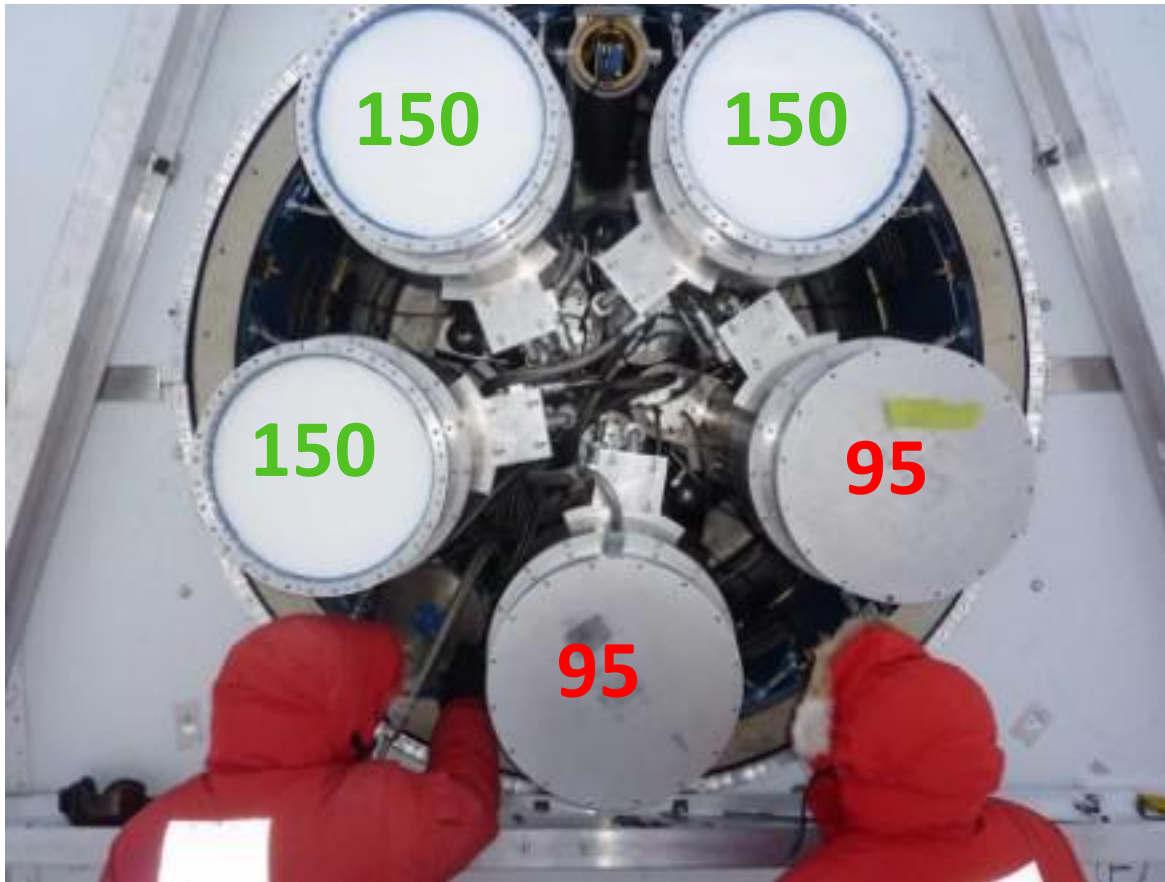
- 2012-2013: All Keck Array receivers at 150 GHz



2012-2013

Keck Array Frequency Coverage

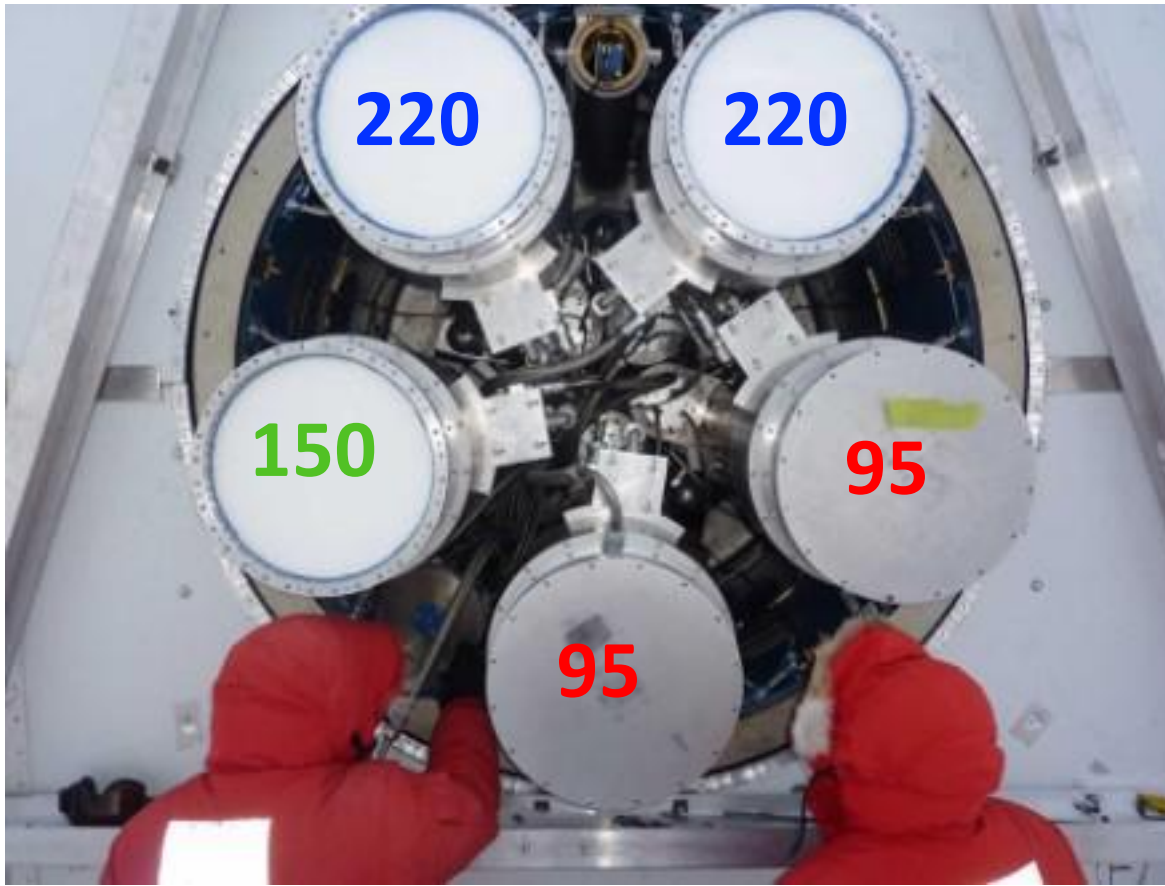
- 2012-2013: All Keck Array receivers at 150 GHz
- 2014: Two 150 GHz receivers replaced with 95 GHz



2014

*BK14: The Keck Array and BICEP2
Collaborations, Phys. Rev. Lett. 116,
031302, 2015*

Keck Array Frequency Coverage



- 2012-2013: All Keck Array receivers at 150 GHz
- 2014: Two 150 GHz receivers replaced with 95 GHz
- 2015: Two additional 150s replaced with 220s

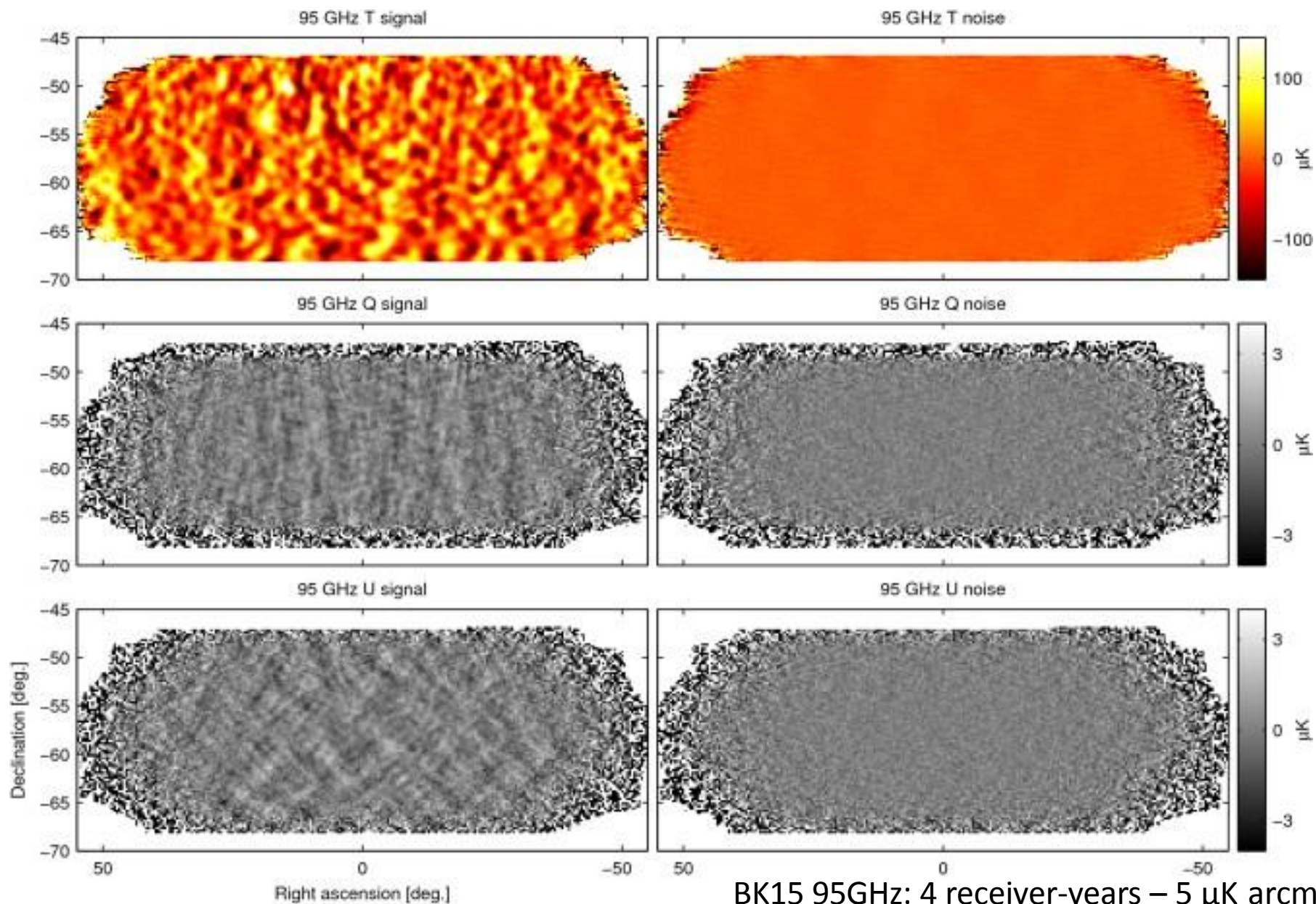
2015

BK15: Out soon!

III.

Results with
data up to 2015

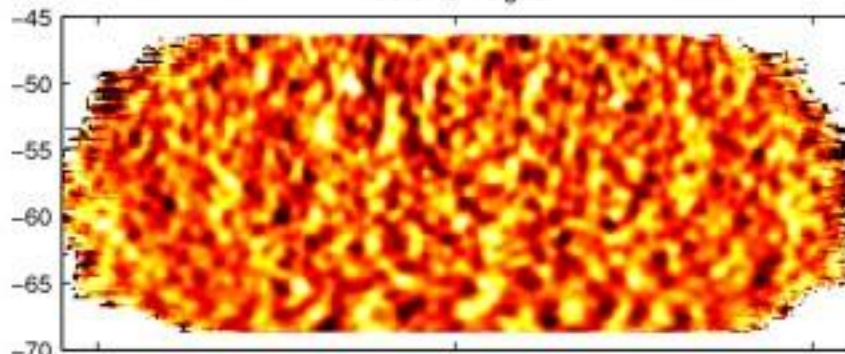
Upcoming BK15 95GHz Maps



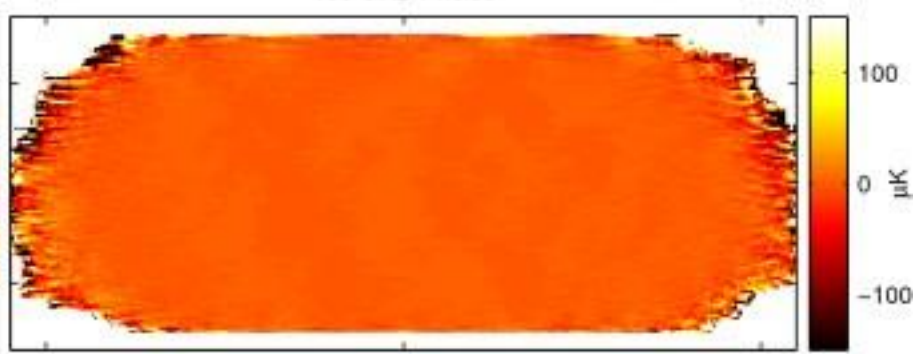
BK15 95GHz: 4 receiver-years – 5 μK arcmin

Upcoming BK15 150GHz Maps

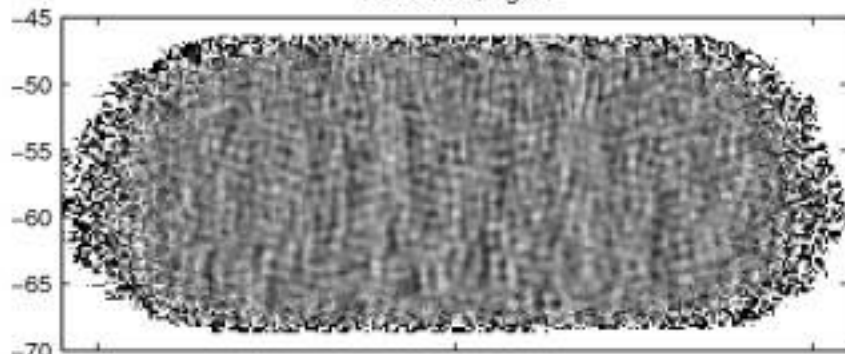
150 GHz T signal



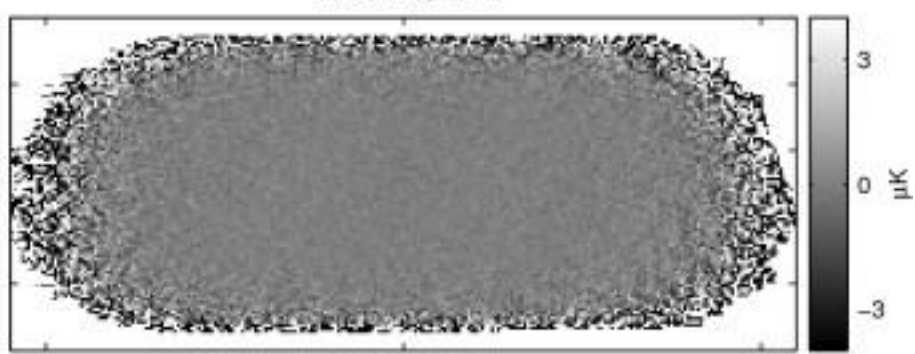
150 GHz T noise



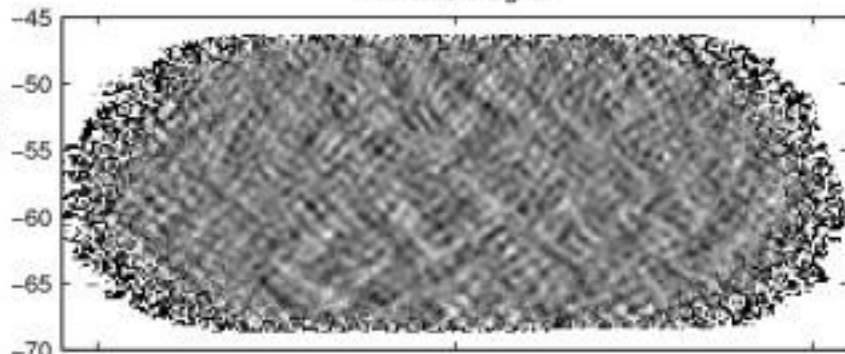
150 GHz Q signal



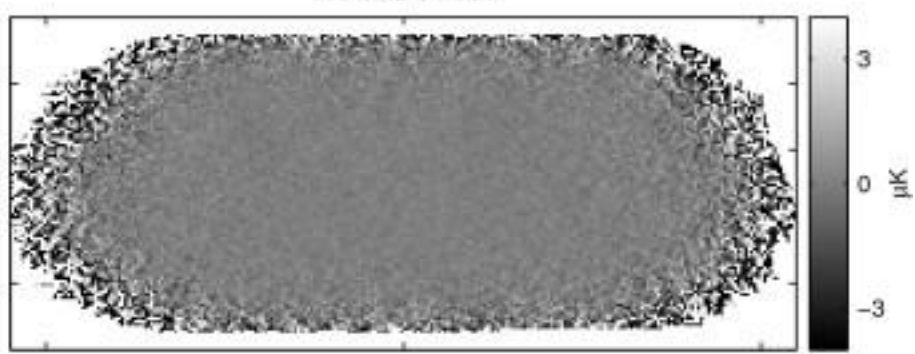
150 GHz Q noise



150 GHz U signal



150 GHz U noise



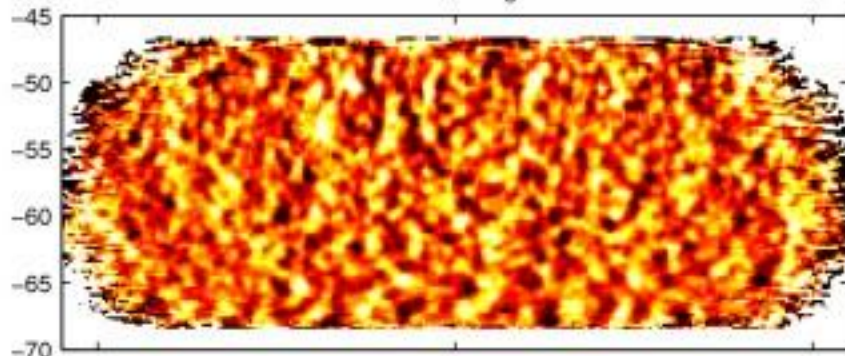
Declination [deg.]

Right ascension [deg.]

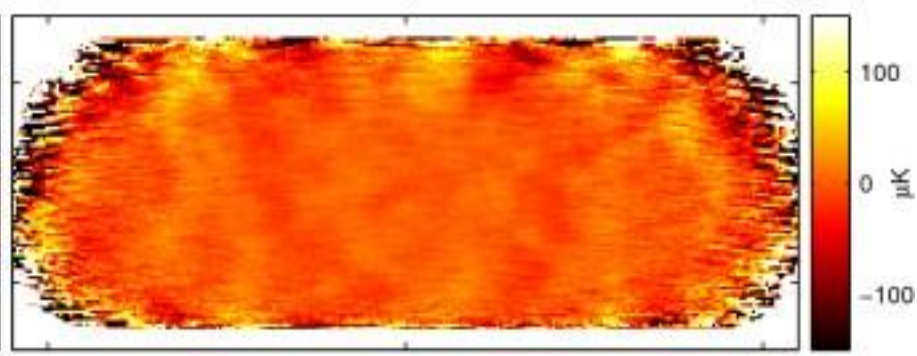
BK15 150GHz: 17 receiver-years – 2.8 μK arcmin

Upcoming BK15 220GHz Maps

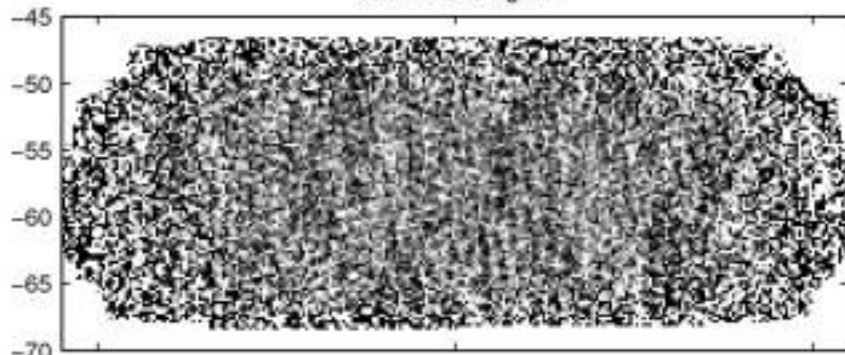
220 GHz T signal



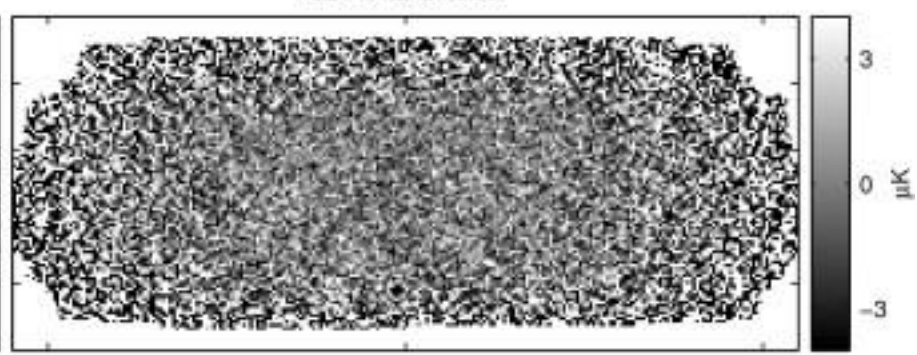
220 GHz T noise



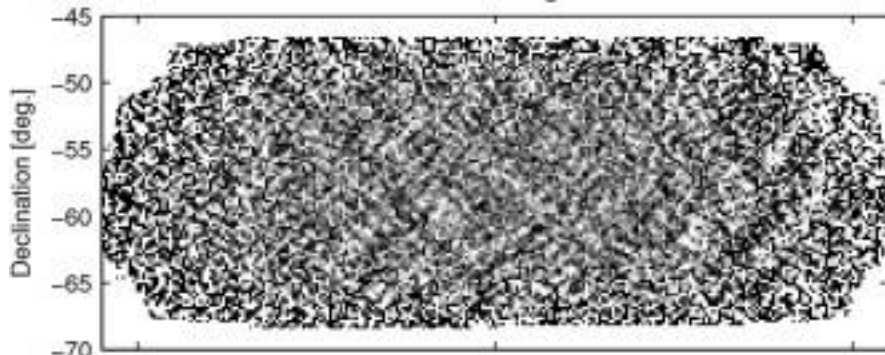
220 GHz Q signal



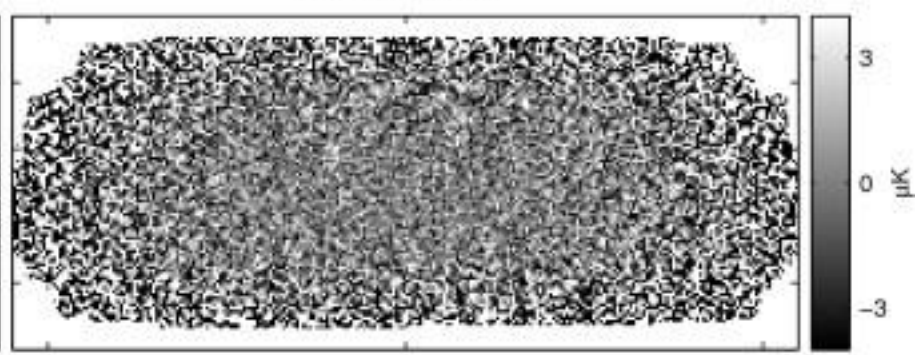
220 GHz Q noise



220 GHz U signal



220 GHz U noise

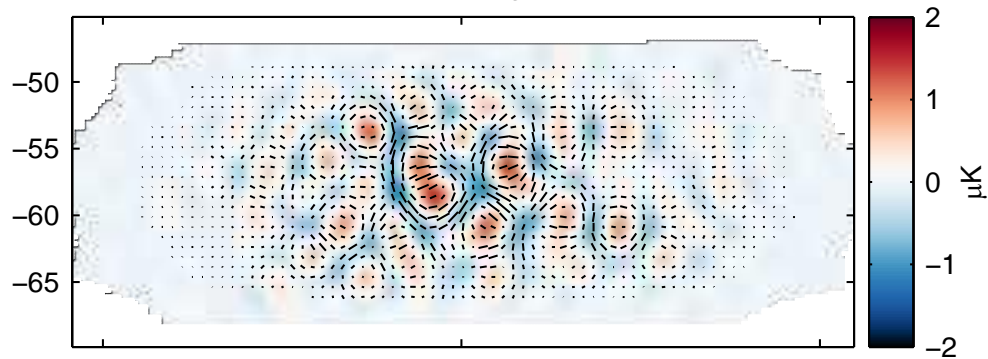


Right ascension [deg.]

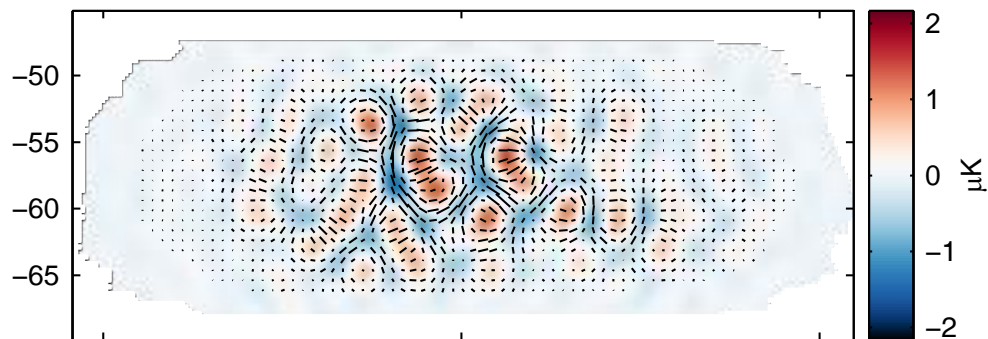
BK15 220GHz- 2 receiver-years – 25 μK arcmin

Upcoming Keck 2015-only E-mode Maps

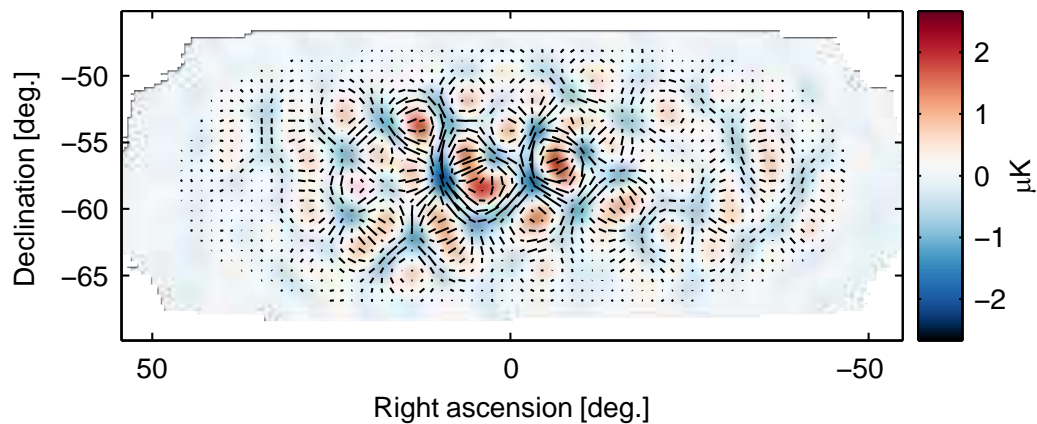
95 GHz E signal



150 GHz E signal

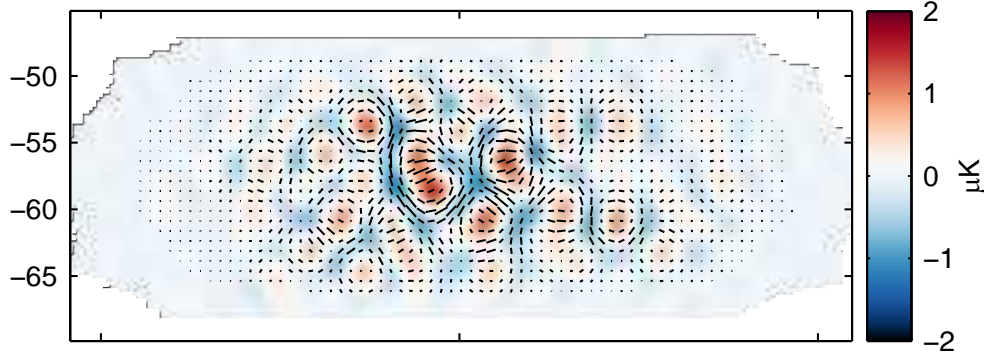


220 GHz E signal

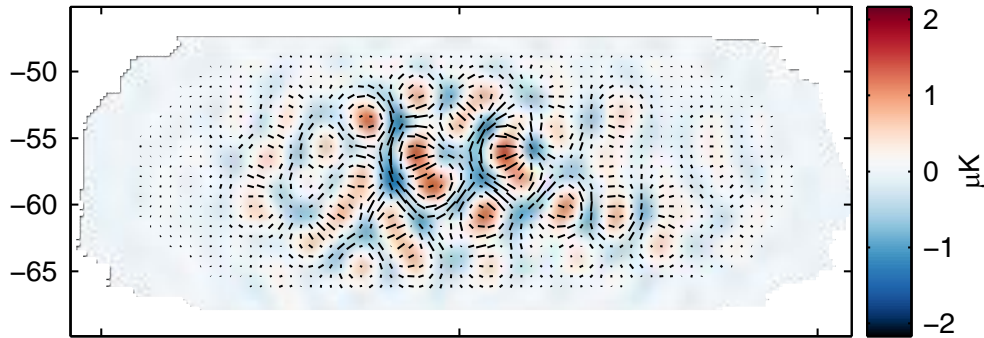


Upcoming Keck 2015-only E-mode Maps

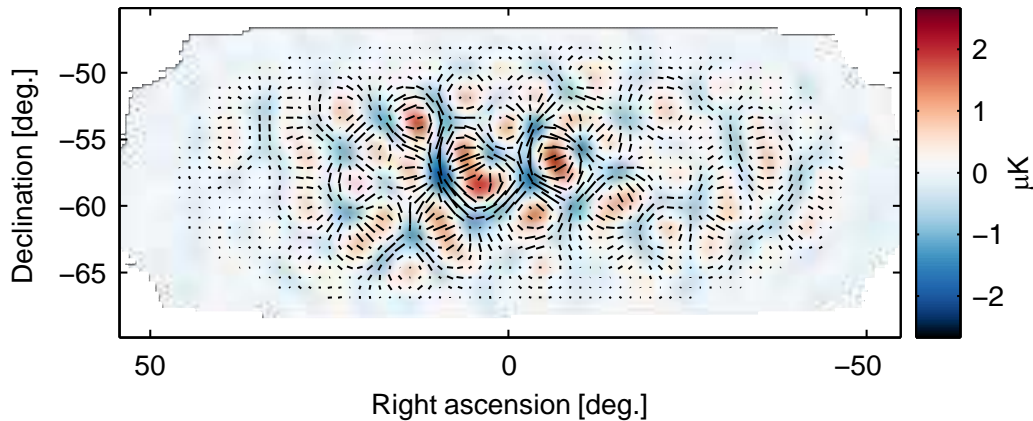
95 GHz E signal



150 GHz E signal

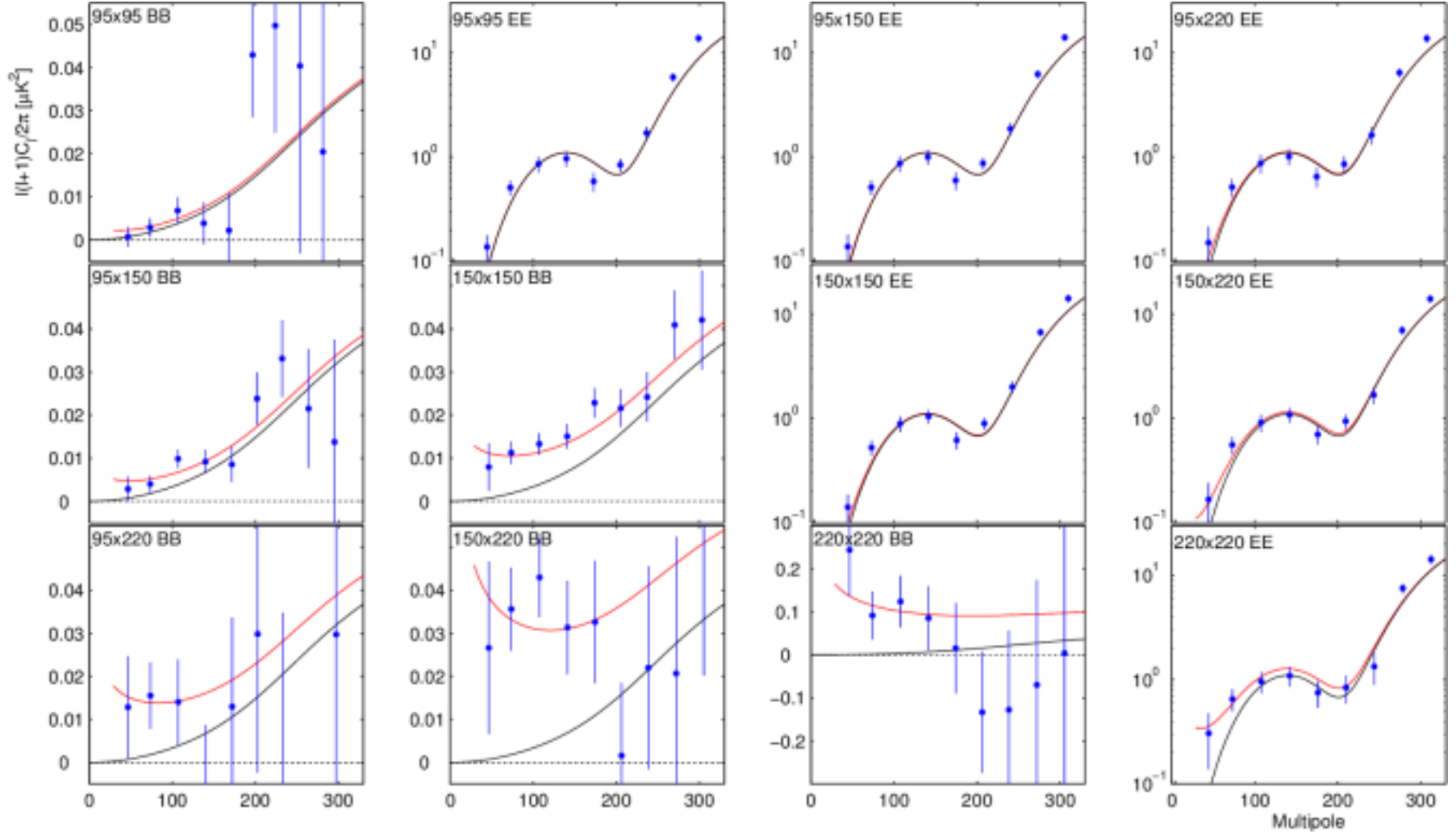


220 GHz E signal



New for BK15
Already 3x deeper than Planck 217 GHz.

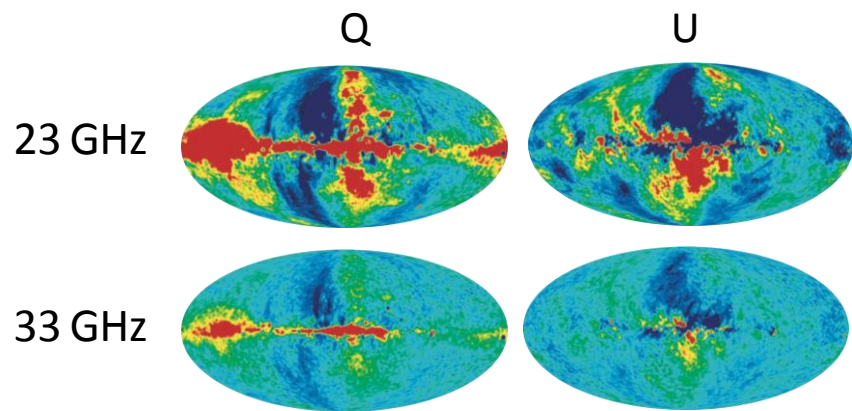
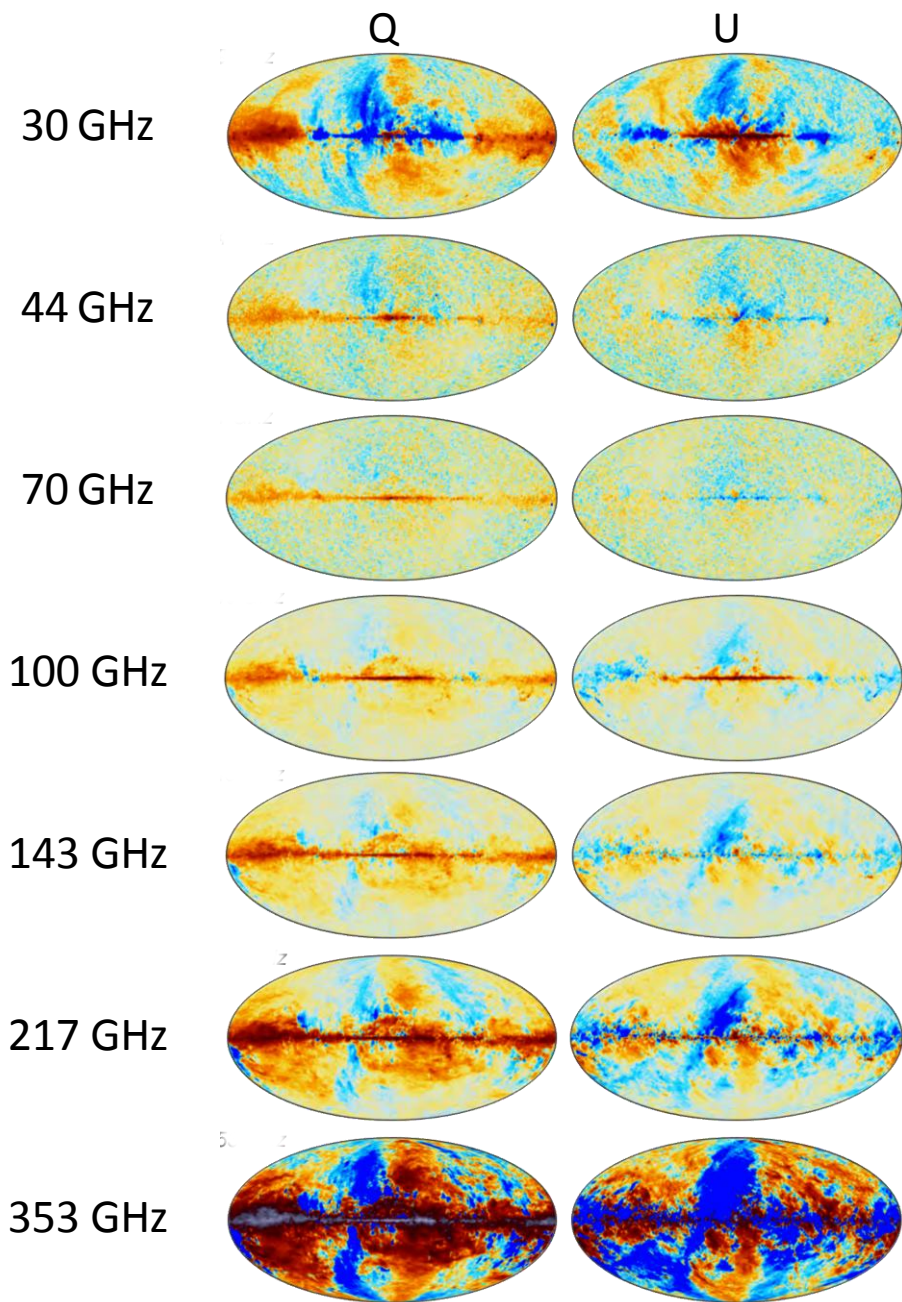
Upcoming BK15 spectra



Spectra using all data up to and including 2015 – adding Keck 220 GHz for the first time.

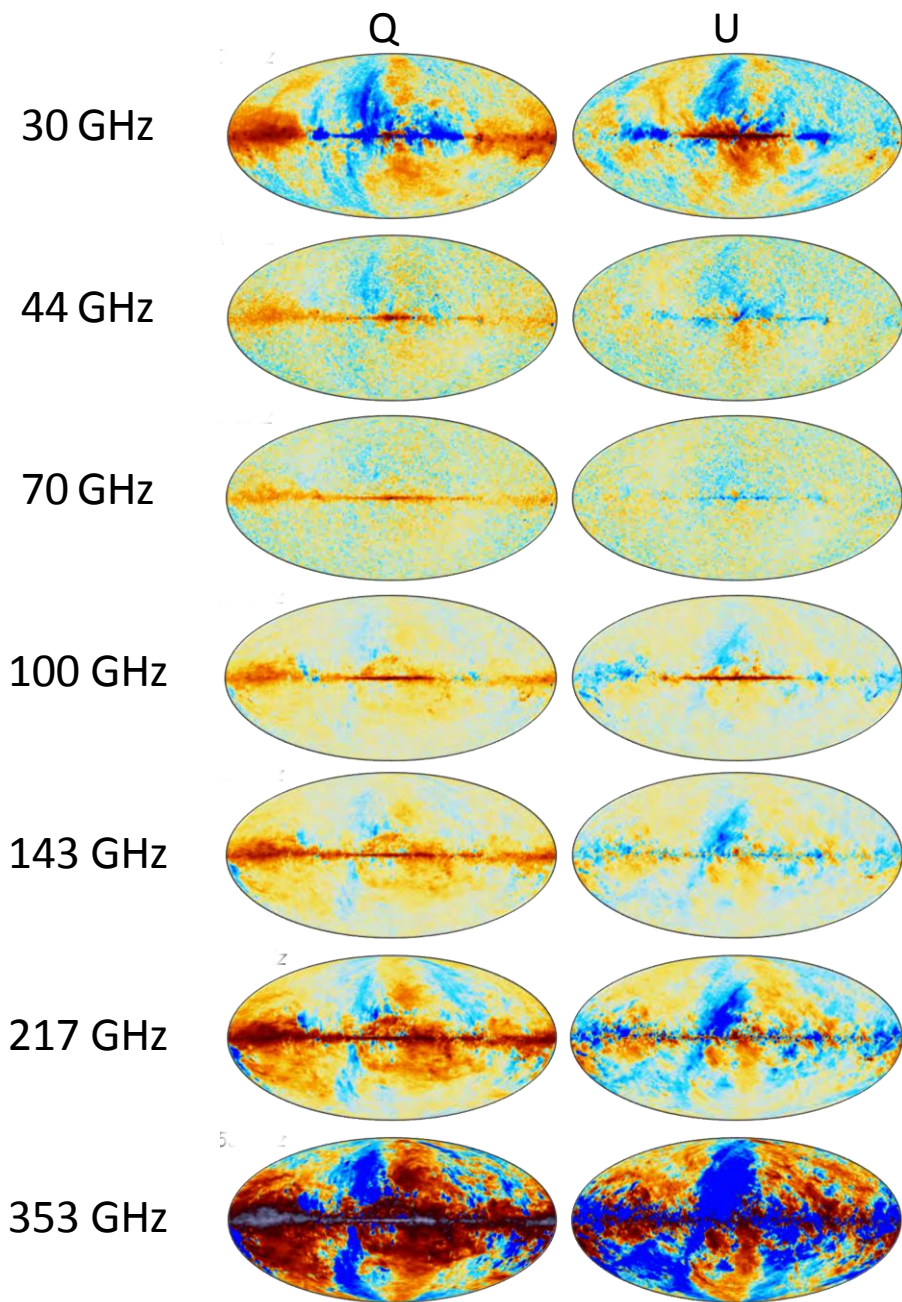
Red line: BK14 baseline model (CMB+polarized dust model with $r = 0$)

Planck polarized maps at 7 frequencies + WMAP at 2 frequencies

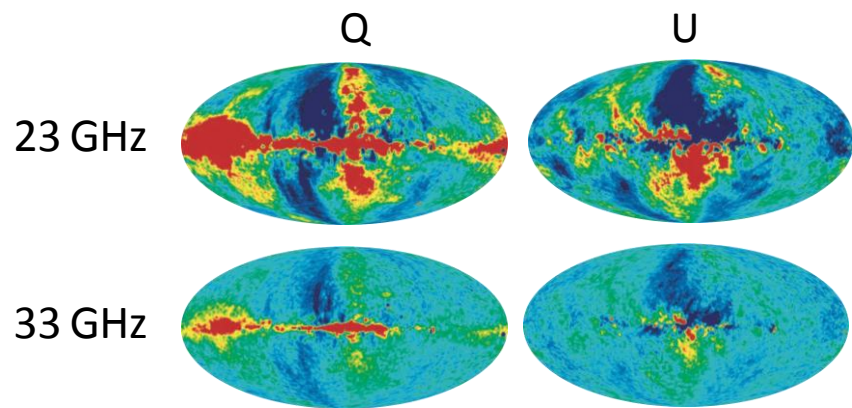


From arxiv 1212.5225

Planck polarized maps at 7 frequencies + WMAP at 2 frequencies



Polarized galactic **synchrotron** emission dominates at low frequencies.



From arxiv 1212.5225

Polarized thermal emission from galactic **dust** dominates at high frequencies.

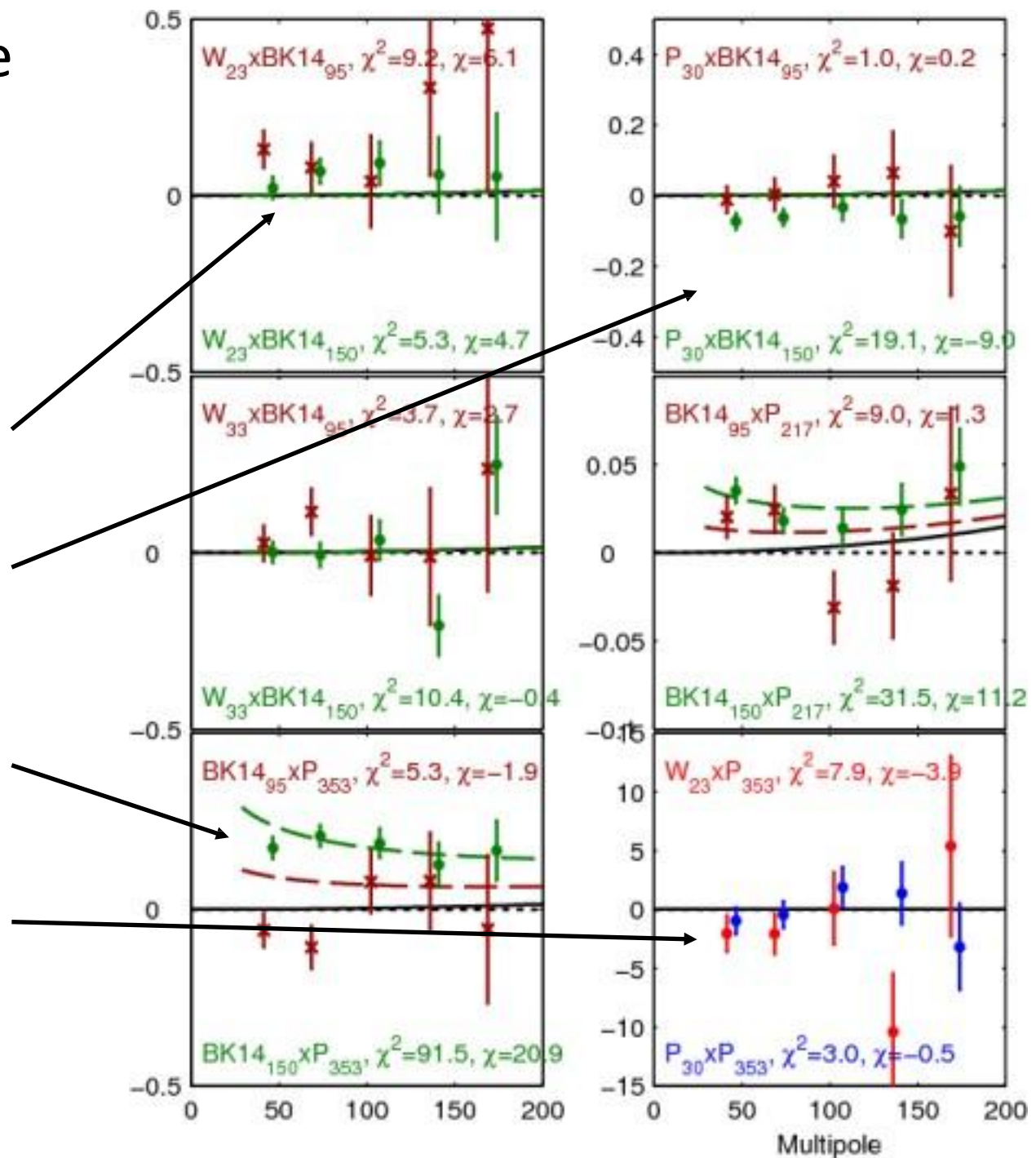
A selected sample of cross spectra between BK and WMAP/Planck

23x150 shows hint of synchrotron,

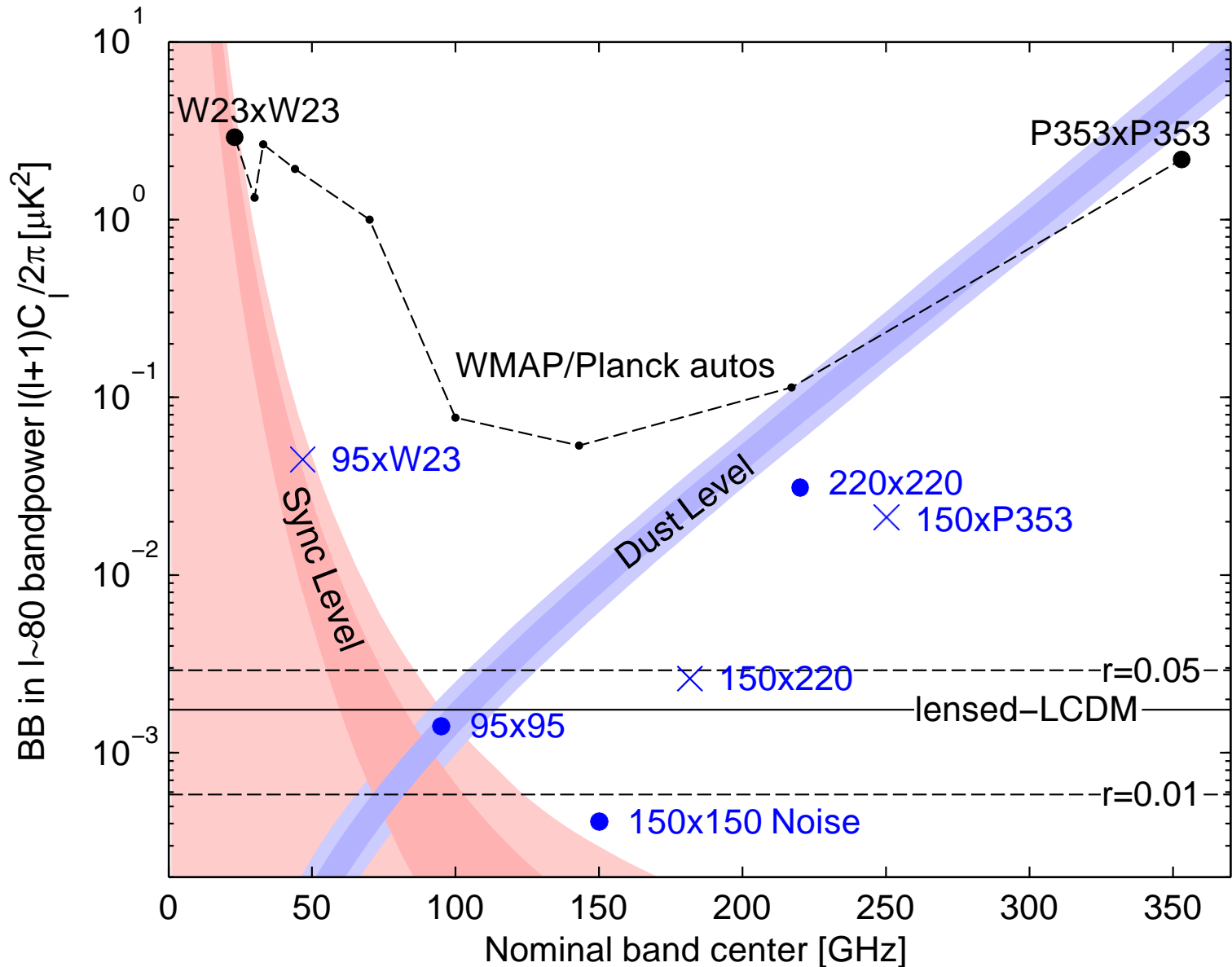
which don't appear in 30x150 .

Strong detection of dust in 150x353

No evidence for dust/sync correlation in 23x353.



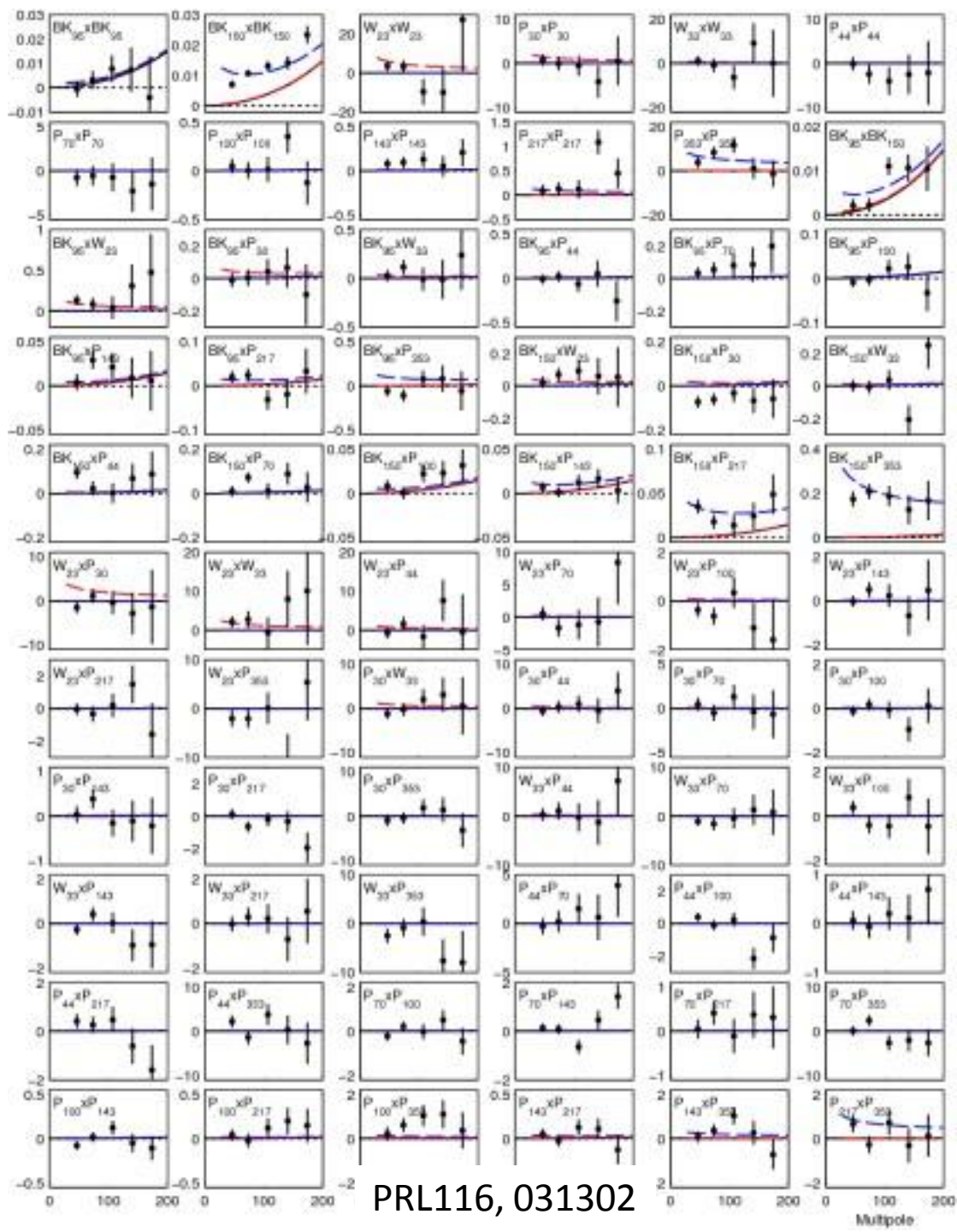
BK15 Band Sensitivity (at $l=80$)



BK14 Auto- and cross- spectra between BICEP/Keck, WMAP, and Planck bands

BK14: 66 spectra

BK15: add 220 GHz \rightarrow 78 spectra



Multicomponent likelihood analysis

Take the joint likelihood of all the spectra simultaneously, vs. model for BB:

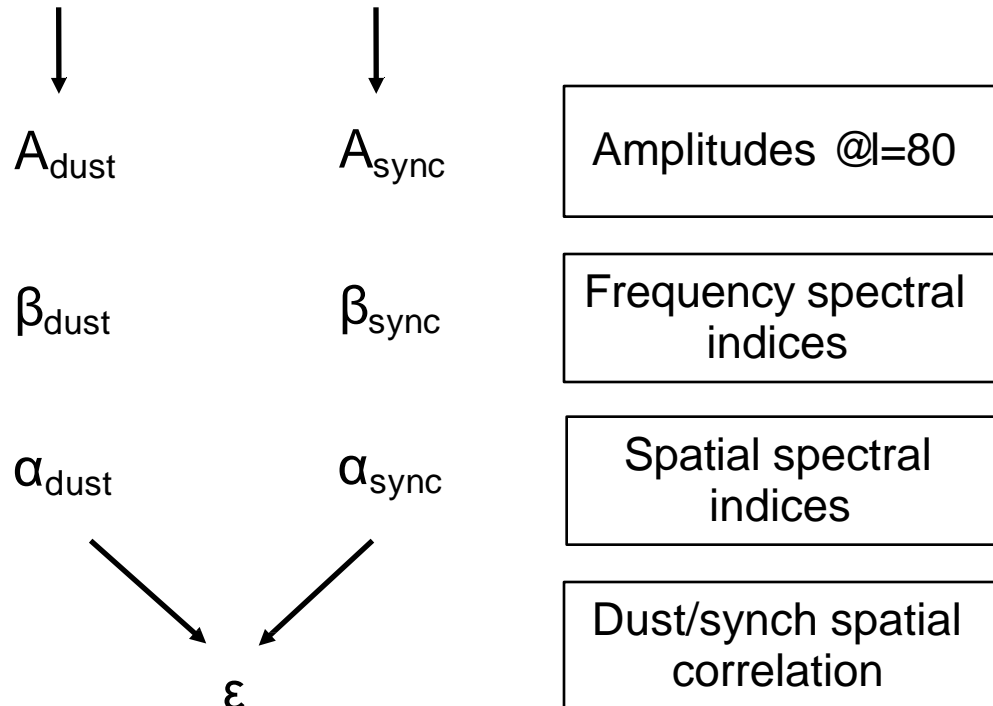
- Expectation for Λ CDM and lensing
- **7-parameter foreground model**
- **r**

Multicomponent likelihood analysis

Take the joint likelihood of all the spectra simultaneously, vs. model for BB:

- Expectation for Λ CDM and lensing
- **7-parameter foreground model**
- **r**

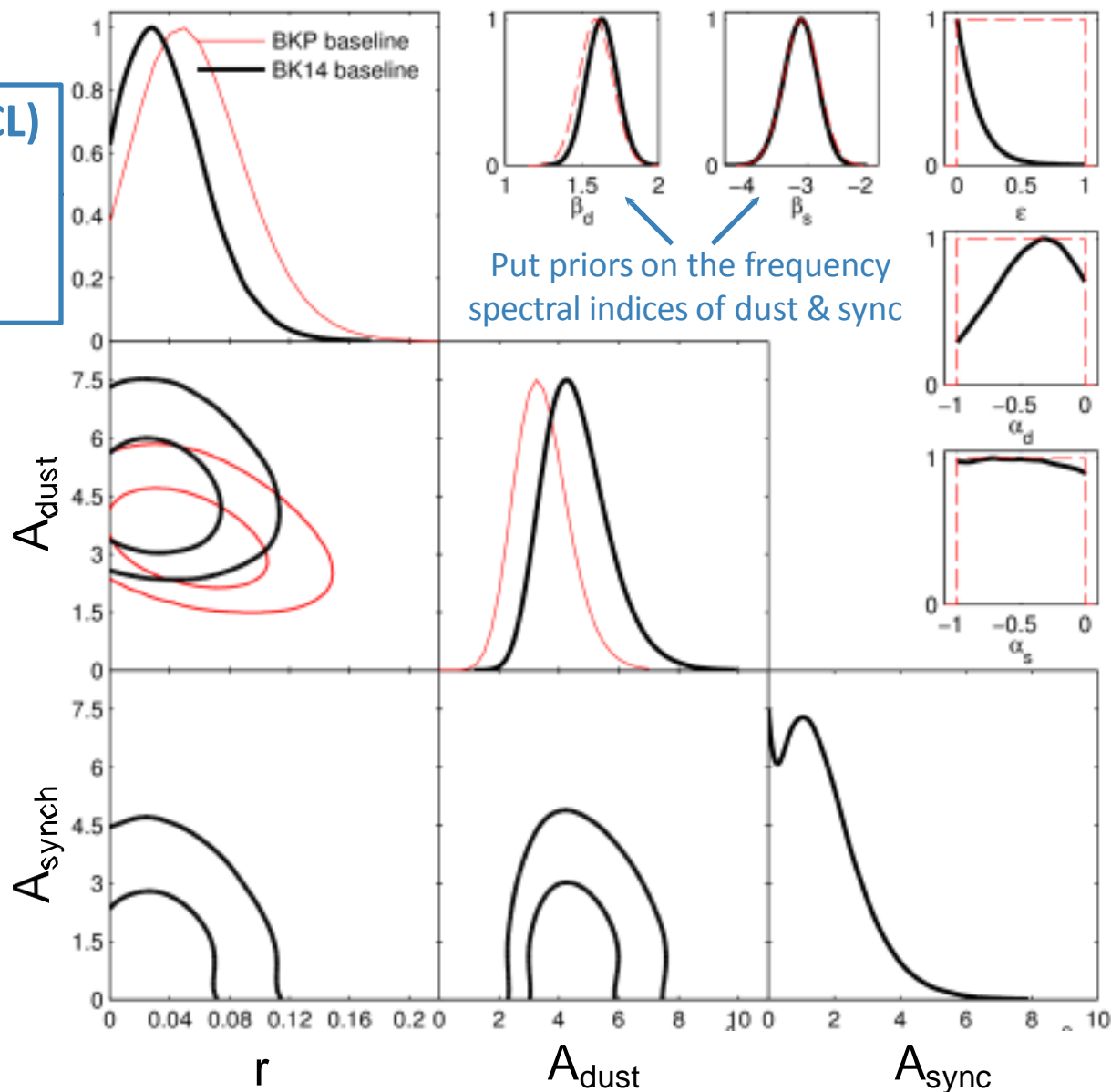
Foreground model = dust + synchrotron



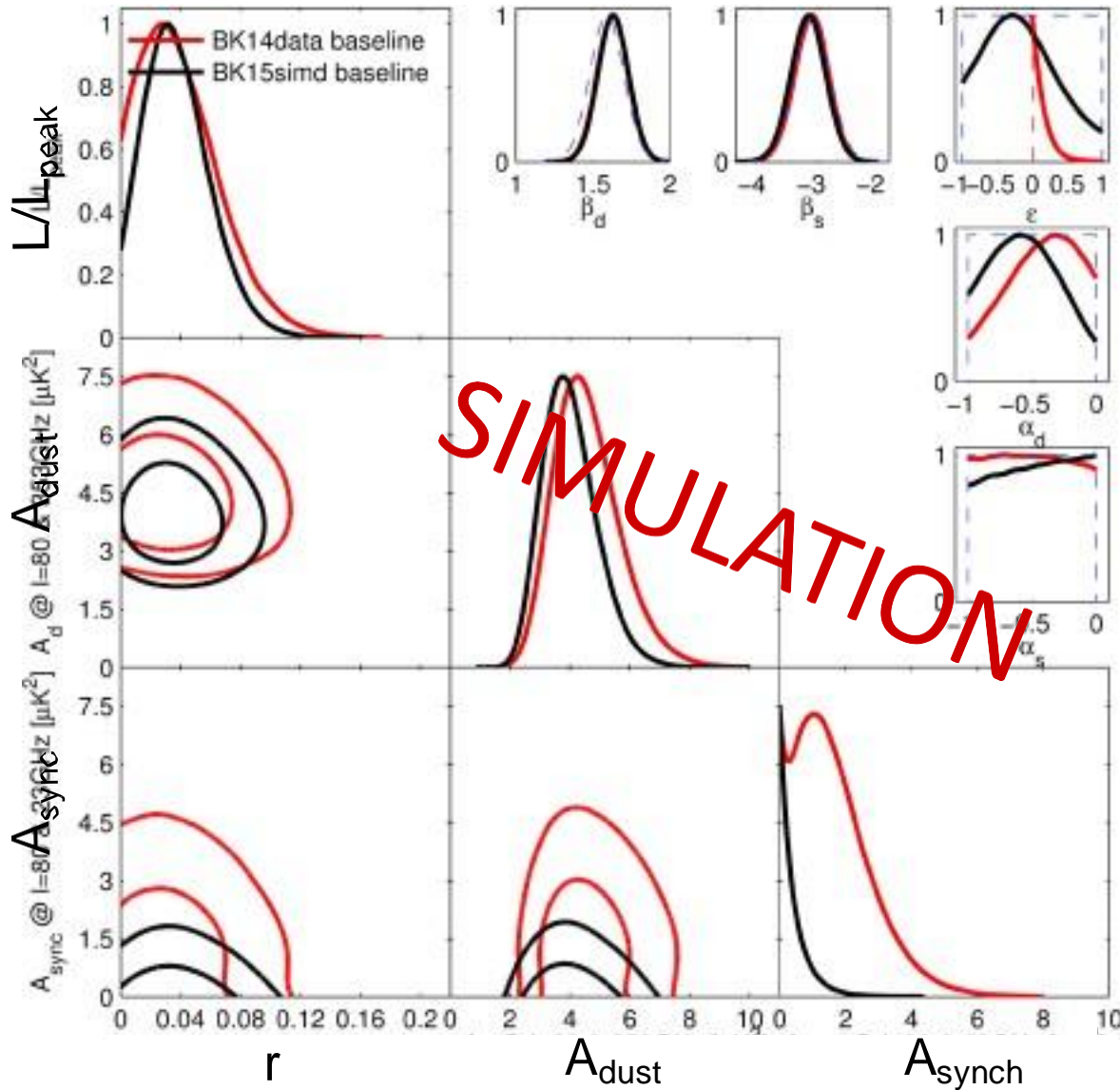
BK14 Results

$r < 0.009$ (95% CL)
Now beats
temperature
constraints

Dust vs. r degeneracy
lifted



BK15 Simulated Results

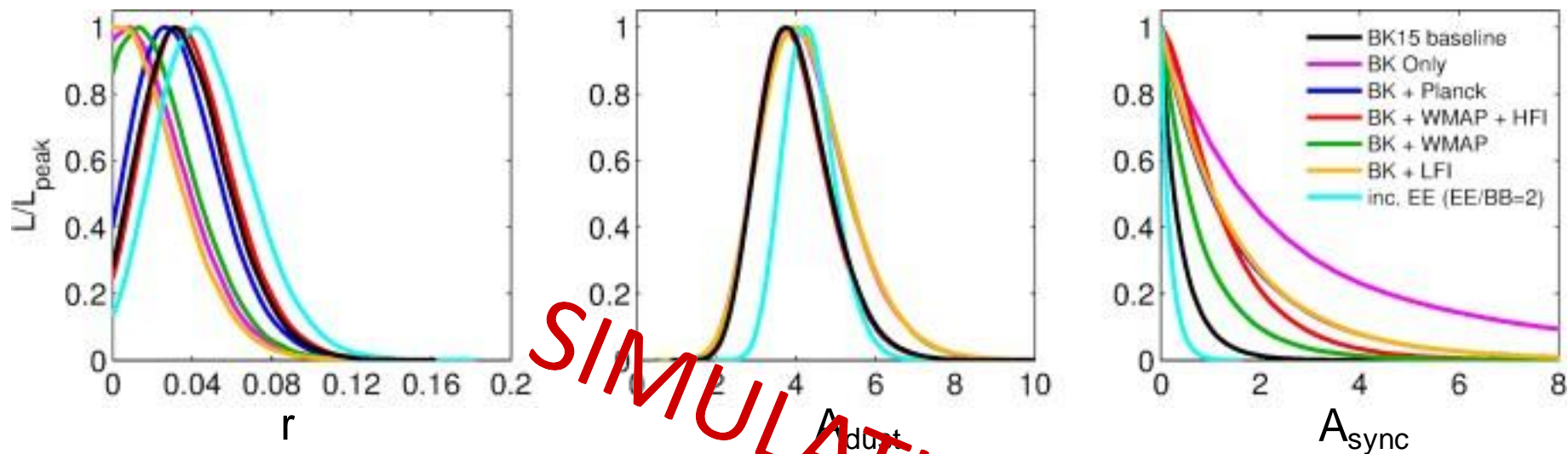


Allow dust/sync correlation, now [-1,1]

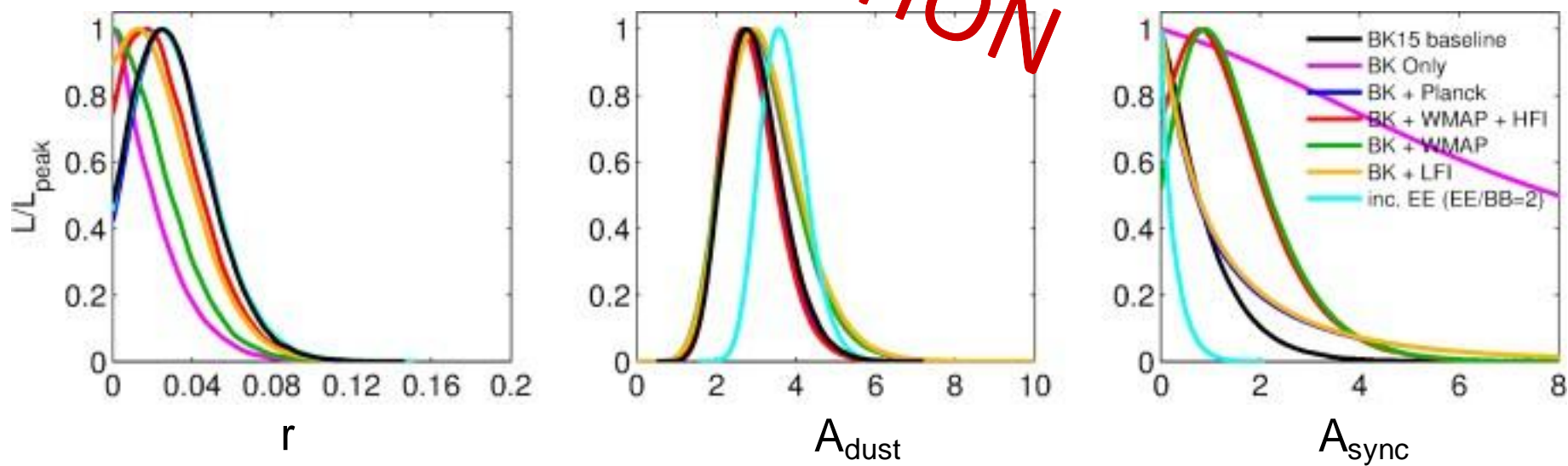
- Plus many alternate analyses presented:
- Foreground priors
 - Including EE
 - WMAP/Planck data
 - Dust decorrelation

BK15 Simulated Results: Variations with Data Selection

BK15 Sim119



BK15 Sim494



SIMULATION

Dust Decorrelation?

Planck 2016

Planck intermediate results. L. Evidence for spatial variation of the polarized thermal dust spectral energy distribution and implications for CMB B-mode analysis

Planck Collaboration: N. Aghanim^{1,2}, M. Ashdown^{3,4}, J. Aumont^{5,6}, C. Bacigalupi^{7,8}, M. Ballardini^{9,10}, A. J. Benabib^{11,12}, R. B. Barreiro¹³, N. Bartolo¹⁴, S. Basil¹⁵, K. Benabib^{16,17}, J. P. Bernard^{18,19}, M. Bernabetti^{20,21}, P. Bevilacqua^{22,23}, A. Bonaldi²⁴, L. Bossera²⁵, J. R. Bond²⁶, J. Borrill^{27,28}, F. R. Braxma²⁹, J. P. Brocard³⁰, E. Boulanger³¹, A. Bracco³², C. Burgatta^{33,34}, E. Calabrese³⁵, J.-F. Cardoso^{36,37}, H. C. Chiang³⁸, L. P. L. Colombo³⁹, C. Combar⁴⁰, B. Comins⁴¹, H. P. Cruikshank⁴², A. Cucchi⁴³, J. Curcio⁴⁴, R. J. Davis⁴⁵, P. de Bernardis⁴⁶, A. de Rosa⁴⁷, G. de Zotti^{48,49}, J. Delabrousse⁵⁰, J.-M. Delouis^{51,52}, E. Di Valentino^{53,54}, C. Dickinson⁵⁵, J. M. Diego⁵⁶, O. Doré^{57,58}, M. Dougan⁵⁹, A. Ducout^{60,61}, X. Dupac⁶², S. Dusini⁶³, G. Efstathiou^{64,65}, F. Elsner^{66,67}, T. A. Enßlin⁶⁸, H. K. Fréchet⁶⁹, F. Fagnano⁷⁰, Y. Farouq^{71,72}, F. Ferrel^{73,74}, M. Frailor⁷⁵, A. A. Fraisse⁷⁶, F. Frascaoli⁷⁷, A. Frolov⁷⁸, S. Galeazzi⁷⁹, S. Galli⁸⁰, K. Ganga⁸¹, R. T. Génova-Santos⁸², M. Gerbasi^{83,84}, T. Ghosh⁸⁵, M. Glend⁸⁶, J. González-Nuevo⁸⁷, K. M. Górski⁸⁸, A. Grappone⁸⁹, J. B. Guberman^{90,91}, J. K. Hammer⁹², G. Helou⁹³, D. Herrero⁹⁴, E. Hiron⁹⁵, Z. Huang⁹⁶, A. H. Jaffe⁹⁷, W. C. Jones⁹⁸, S. Kabana⁹⁹, R. Karkhaneh¹⁰⁰, T. S. Knaflitz¹⁰¹, N. Krachwalinski¹⁰², M. Kosa¹⁰³, H. Korki-Saarni¹⁰⁴, G. Lagache¹⁰⁵, A. Lahav^{106,107}, J.-M. Lamarca¹⁰⁸, A. Lacey¹⁰⁹, M. Lattanzi¹¹⁰, C. R. Lawrence¹¹¹, M. Le Jeune¹¹², F. Levrier¹¹³, M. Liguori¹¹⁴, P. B. Lilje¹¹⁵, M. López-Carrión¹¹⁶, P. M. Lubin¹¹⁷, J. F. Macías-Pérez¹¹⁸, G. Maggio¹¹⁹, D. Maino¹²⁰, N. Mandoulas¹²¹, A. Mangano¹²², M. Marin¹²³, P. G. Martin¹²⁴, E. Martínez-González¹²⁵, S. Matsumoto^{126,127}, N. Maffei¹²⁸, J. D. Mather¹²⁹, A. Meneilly¹³⁰, A. Menisetti¹³¹, M. Migliaccio¹³², S. Mitra¹³³, M.-A. Miville-Deschênes¹³⁴, D. Molinaro^{135,136}, A. Moneti¹³⁷, L. Monier¹³⁸, G. Morgante¹³⁹, A. Moss¹⁴⁰, P. Nasiryan¹⁴¹, H. U. Nørgaard-Nielsen¹⁴², C. A. O'Hare¹⁴³, L. Pagano¹⁴⁴, D. Paoletti¹⁴⁵, B. Patridge¹⁴⁶, L. Parris¹⁴⁷, O. Perdereau¹⁴⁸, L. Perotto¹⁴⁹, V. Petrosian¹⁵⁰, F. Piacentini¹⁵¹, S. Planck¹⁵², G. Polenta¹⁵³, J.-L. Puget¹⁵⁴, J. P. Rachen¹⁵⁵, M. Reinecke¹⁵⁶, M. Remazeilles^{157,158}, A. Renzi¹⁵⁹, G. Resseis¹⁶⁰, M. Rossetti¹⁶¹, G. Roudot^{162,163}, J. A. Rubiño-Martín¹⁶⁴, H. Riso-Gracía¹⁶⁵, E. Sefrioui¹⁶⁶, M. Saitoh¹⁶⁷, M. Savellani¹⁶⁸, D. Scaife¹⁶⁹, C. Scrimgeour¹⁷⁰, G. Serri¹⁷¹, I. Stancu¹⁷², J.-S. Sunm¹⁷³, J. A. Tague¹⁷⁴, M. Tenzel¹⁷⁵, L. Toffanti^{176,177}, M. Tomasi¹⁷⁸, M. Tramacchi¹⁷⁹, J. Valiviita¹⁸⁰, E. Vanzura¹⁸¹, J. Van Weeren¹⁸², P. Vielva¹⁸³, R. D. Weiler^{184,185}, I. K. Wehus¹⁸⁶, A. Zacher¹⁸⁷, and A. Zonca¹⁸⁸

(Affiliations can be found after the references)

Preprint online version: June 24, 2016

ABSTRACT

The characterization of the Galactic foregrounds has been shown to be the main obstacle in the challenging quest to detect primordial B-modes in the polarized microwave sky. We make use of the Planck-PR3 2013 data release at high frequencies to place new constraints on the properties of the polarized thermal dust emission at high Galactic latitudes. Here, we specifically study the spatial variability of the dust polarized spectral energy distribution (SED), and its potential impact on the determination of the tensor-to-scalar ratio, r . We use the correlation ratio of the $l^{2\alpha}$ angular power spectra between the 217- and 353-GHz channels as a tracer of these potential variations, computed on different high Galactic latitude regions, ranging from 80% to 20% of the sky. The new insight from Planck data is a departure of the correlation ratio from unity that cannot be attributed to a spurious decorrelation due to the cosmic microwave background, instrumental noise, or interstellar systematics. The effect is marginally detected on each region, but the statistical combination of all the regions gives more than 99% confidence for this variation in polarized dust properties. In addition, we show that the decorrelation increases when there is a decrease in the mean column density of the region of the sky being considered, and we propose a simple power-law empirical model for this dependence, which matches what is seen in the Planck data. We explore the effect that this measured decorrelation has on simulations of the BICEP2-Keck Array/Suzuki analysis and show that the 2013 constraints from those data still allow a decorrelation between the data at 150 and 353 GHz of the order of the one we measure. Finally, using simplified models, we show that either spatial variation of the dust SED or of the dust polarization angle could produce decorrelations between 217- and 353-GHz data similar to those we observe in the data.

A departure of the correlation ratio from unity that cannot be attributed to a spurious decorrelation due to the cosmic microwave background, instrumental noise, or instrumental systematics... **detected at more than 99% confidence**

Planck 2018

Planck intermediate results. LIV. Polarized dust foregrounds

Planck Collaboration: Y. Akram^{1,2}, M. Ashdown^{3,4}, J. Aumont⁵, C. Bacigalupi^{6,7}, M. Ballardini^{8,9}, A. J. Benabib^{10,11}, R. B. Barreiro¹², N. Bartolo¹³, S. Basil¹⁴, K. Benabib^{15,16}, J. P. Bernard^{17,18}, M. Bernabetti^{19,20}, P. Bevilacqua^{21,22}, J. R. Bond²³, J. Borrill²⁴, F. R. Braxma²⁵, L. Bossera²⁶, A. Bracco²⁷, M. Bucher²⁸, C. Burgatta^{29,30}, E. Calabrese³¹, J.-J. Cardoso³², J. Carron³³, H. C. Chiang³⁴, C. Combar³⁵, H. P. Cruikshank³⁶, P. de Bernardis³⁷, G. de Zotti^{38,39}, J. Delabrousse⁴⁰, J.-M. Delouis^{41,42}, E. Di Valentino^{43,44}, C. Dickinson⁴⁵, J. M. Diego⁴⁶, A. Ducout⁴⁷, X. Dupac⁴⁸, F. Elsner⁴⁹, T. A. Enßlin⁵⁰, D. Falgarone⁵¹, Y. Farouq⁵², K. Ferrise⁵³, J. Ferrel⁵⁴, J. Ferrière⁵⁵, M. Frailor⁵⁶, A. A. Fraisse⁵⁷, F. Frascaoli⁵⁸, A. Frolov⁵⁹, S. Galeazzi⁶⁰, S. Galli⁶¹, K. Ganga⁶², R. T. Génova-Santos⁶³, T. Ghosh⁶⁴, J. González-Nuevo⁶⁵, K. M. Górski⁶⁶, A. Grappone⁶⁷, J. B. Guberman^{68,69}, J. K. Hammer⁷⁰, W. Handley⁷¹, E. K. Hammer⁷², D. Herrero⁷³, Z. Huang⁷⁴, A. H. Jaffe⁷⁵, W. C. Jones⁷⁶, S. Kabana⁷⁷, R. Karkhaneh⁷⁸, S. Knaflitz⁷⁹, J. Knaflitz⁸⁰, N. Krachwalinski⁸¹, M. Kosa⁸², H. Korki-Saarni⁸³, G. Lagache⁸⁴, A. Lahav⁸⁵, J.-M. Lamarca⁸⁶, A. Lacey⁸⁷, M. Lattanzi⁸⁸, C. R. Lawrence⁸⁹, M. Le Jeune⁹⁰, F. Levrier⁹¹, M. Liguori⁹², P. B. Lilje⁹³, V. Lindholm⁹⁴, M. López-Carrión⁹⁵, P. M. Lubin⁹⁶, Y.-Z. Ma^{97,98}, J. F. Macías-Pérez⁹⁹, G. Maggio¹⁰⁰, D. Maino¹⁰¹, N. Mandoulas¹⁰², A. Mangano¹⁰³, P. G. Martin¹⁰⁴, E. Martínez-González¹⁰⁵, S. Matsumoto^{106,107}, J. D. Mather¹⁰⁸, H. K. Moseley¹⁰⁹, A. Moneti¹¹⁰, M. Migliaccio¹¹¹, M.-A. Miville-Deschênes¹¹², D. Molinaro^{113,114}, A. Moneti¹¹⁵, L. Monier¹¹⁶, G. Morgante¹¹⁷, F. Nasiryan¹¹⁸, L. Pagano¹¹⁹, D. Paoletti¹²⁰, V. Petrosian¹²¹, F. Piacentini¹²², G. Polenta¹²³, J. P. Rachen¹²⁴, M. Reinecke¹²⁵, M. Remazeilles¹²⁶, A. Renzi¹²⁷, G. Resseis¹²⁸, C. Rossetti¹²⁹, J. A. Rubiño-Martín¹³⁰, B. Riso-Gracia¹³¹, E. Sefrioui¹³², J. D. Soker¹³³, L. D. Spencer¹³⁴, J. A. Tague¹³⁵, D. Tenzel¹³⁶, J. Toffanti¹³⁷, M. Tomasi¹³⁸, T. Tramacchi^{139,140}, J. Valiviita¹⁴¹, E. Vanzura¹⁴², J. Van Weeren¹⁴³, P. Vielva¹⁴⁴, P. Vila¹⁴⁵, N. Vittorio¹⁴⁶, I. K. Wehus¹⁴⁷, A. Zacher¹⁴⁸, and A. Zonca¹⁴⁹

(Affiliations can be found after the references)

Preprint online version: January 17, 2018

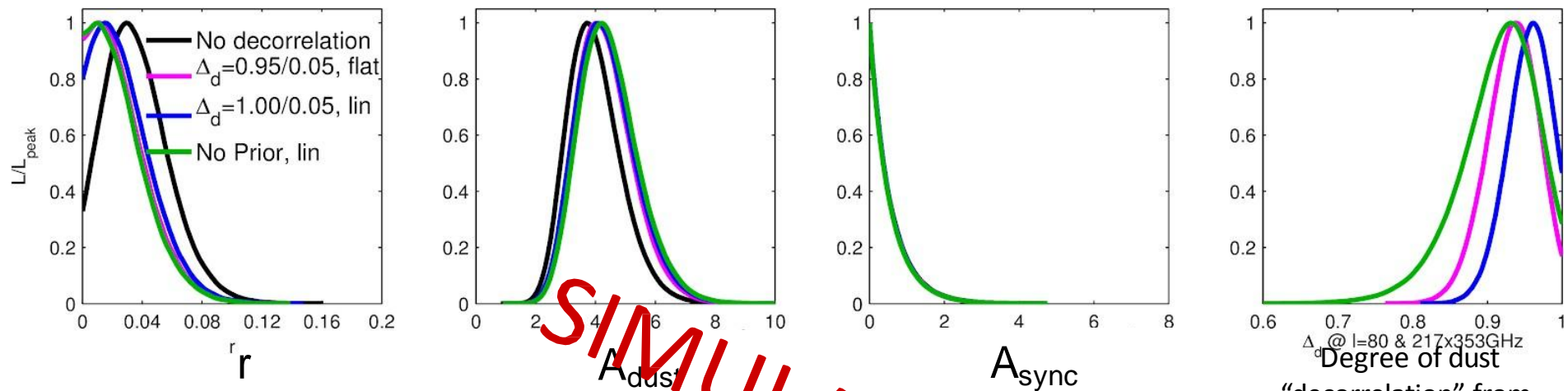
ABSTRACT

The study of polarized dust emission has become essential with the analysis of the cosmic microwave background (CMB) polarization in the quest for the dust-like B-mode polarization from primordial gravitational waves and the low-multipole B-mode polarization associated with the ionization of the Universe. We use the new Planck-PR3 2017 maps to characterize Galactic dust emission at high latitudes as a foreground to the CMB polarization and use end-to-end simulations to compare uncertainties and assess the statistical significance of our measurements. We present Planck $l \ell$, lB , and TB power spectra of dust polarization at 353 GHz for a set of six nested high-Galactic latitude sky regions covering from 24 to 71% of the sky. We present power-law fits to the angular power spectra, yielding evidence for statistically significant variations of the exponents over sky regions and a difference between the values for the lB and lB spectra, which for the largest sky region are $\alpha_{lB} = -2.42 \pm 0.02$ and $\alpha_{lB} = -2.54 \pm 0.02$, respectively. The spectra show that the TB correlation and lTB power asymmetry discovered by Planck extend to low multipoles that were not included in earlier Planck polarization papers due to unresolved dust systematics. We also report evidence for a positive TB dust signal. Combining data from Planck and WMAP, we determine the amplitudes and spectral energy distributions (SEDs) of polarized foregrounds, including the correlation between dust and synchrotron polarized emission, for the six sky regions as a function of multipole. This quantifies the challenge of the component-separation procedure that is required for measuring the low- l ionization CMB E-mode signal and detecting the reionization and recombination peaks of primordial CMB B-modes. The SED of polarized dust emission is fit well by a single-temperature modified blackbody emission law from 250 GHz to below 70 GHz. For a dust temperature of 19.6 K, the mean dust spectral index for dust polarization is $\beta_p = 1.53 \pm 0.02$. The difference between indices for polarization and total intensity is $\beta_p - \beta_t = 0.05 \pm 0.01$. By fitting multi-frequency cross-spectra between Planck data at 100, 143, 217, and 353 GHz, we examine the evolution of the dust polarization maps across frequency. We find no evidence for a loss of correlation and provide lower limits to the correlation ratio that are tighter than values we derive from the correlation of the 217- and 353-GHz maps alone. If the Planck limit on decorrelation for the largest sky region applies to the smaller sky regions observed by sub-orbital experiments, then frequency decorrelation of dust polarization might not be a problem for CMB experiments aiming at a primordial B-mode detection limit at the tensor-to-scalar ratio $r = 0.01$ at the recombination peak. However, the Planck sensitivity prediction identifying how difficult the component separation problem will be for more ambitious experiments targeting lower limits on r .

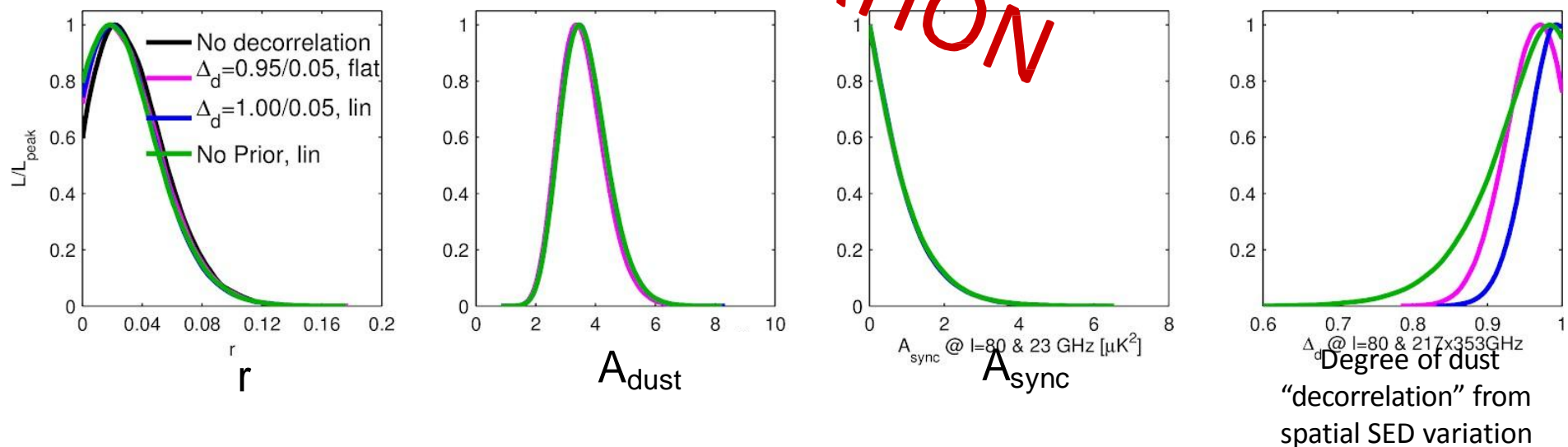
We find no evidence for a loss of correlation.
... might not be a problem for CMB experiments aiming at a primordial B-mode detection limit on the tensor-to-scalar ratio $r \sim 0.01$...

BK15 Simulated Results: Variations with Dust Modeling

BK15 Sim119



BK15 Sim266



SIMULATION

IV.

What's Next?

BICEP3 and BICEP Array

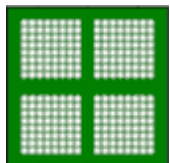
B3: Transition to 500mm-class receiver

Fully 95 GHz

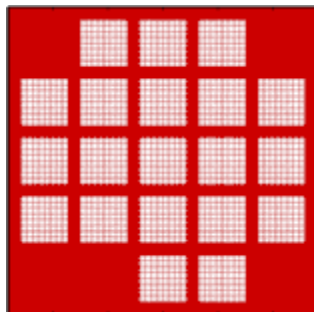
2560 detectors in modular focal plane.

Large-aperture optics and infrared filtering.

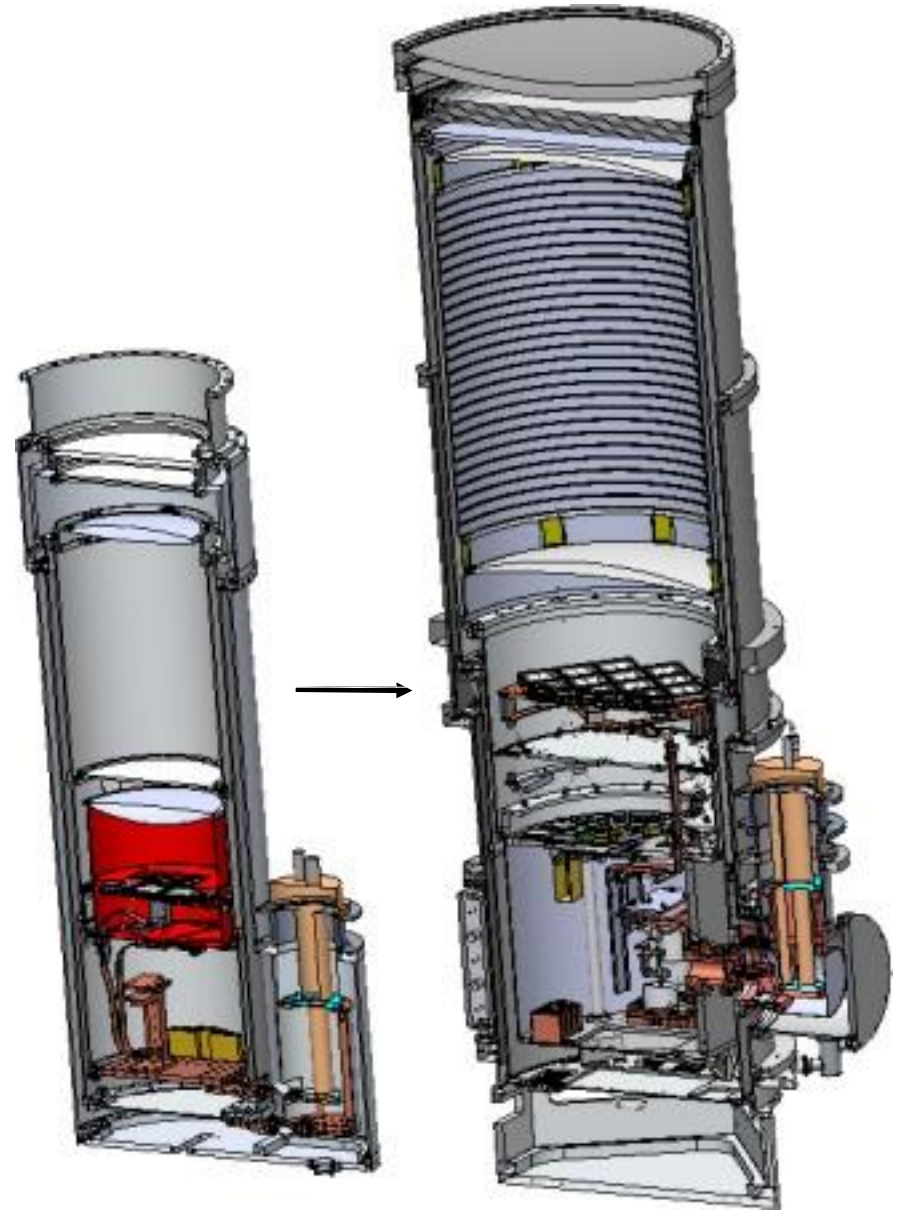
10x optical throughput of single BICEP2/Keck receiver.



BICEP2 FPU



BICEP3

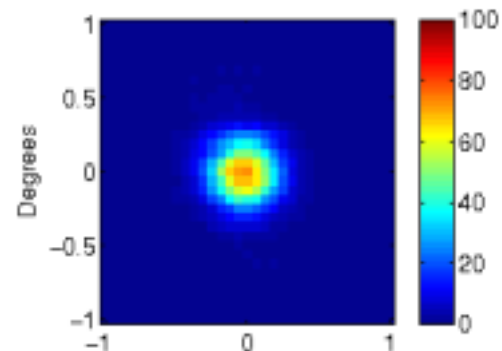


Keck receiver

BICEP3

BICEP3 receiver

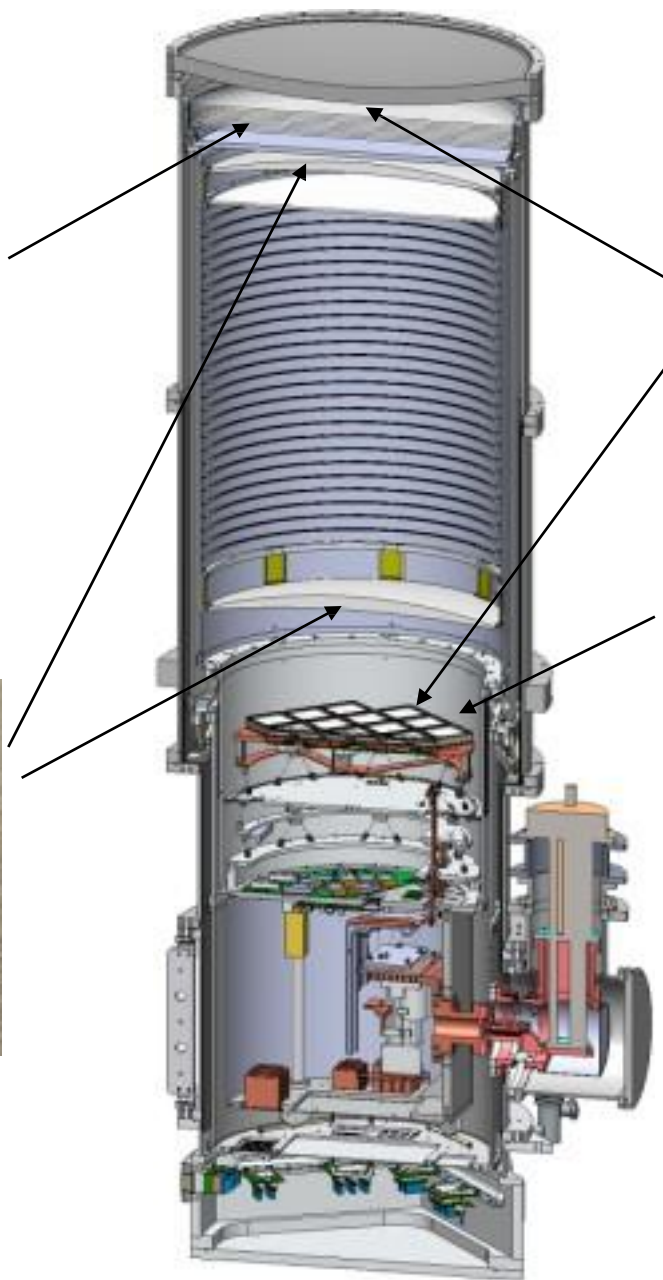
Zotefoam IR reflective filter stack



680-mm clear aperture window,
fast optics (f/1.6), FOV $\sim 28^\circ$
95 GHz beam FWHM $\sim 0.35^\circ$

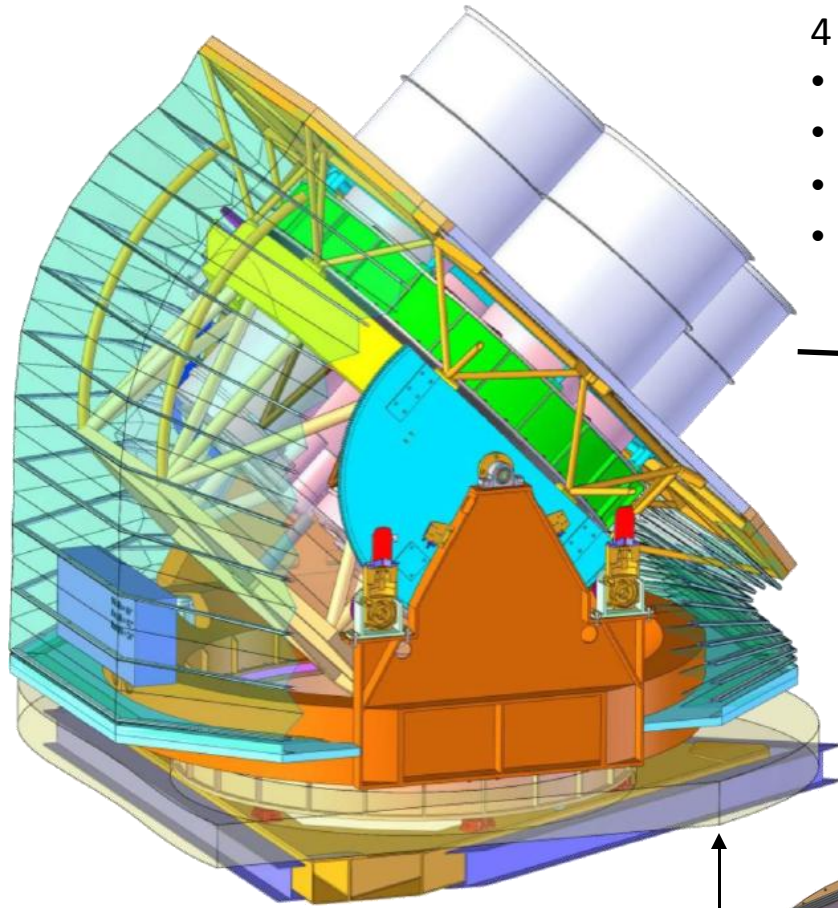


Thin, low loss, high thermal conductivity alumina filters and lenses with epoxy-based antireflection coating.



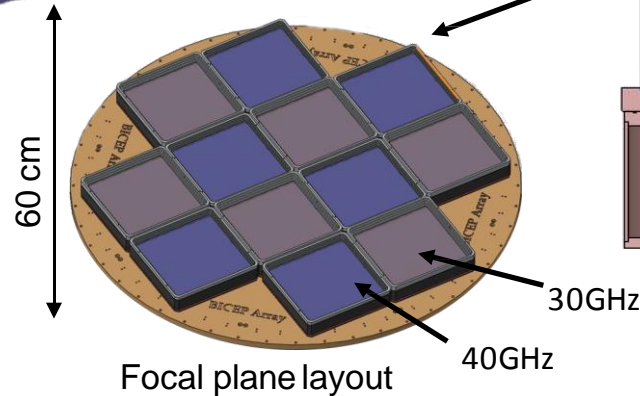
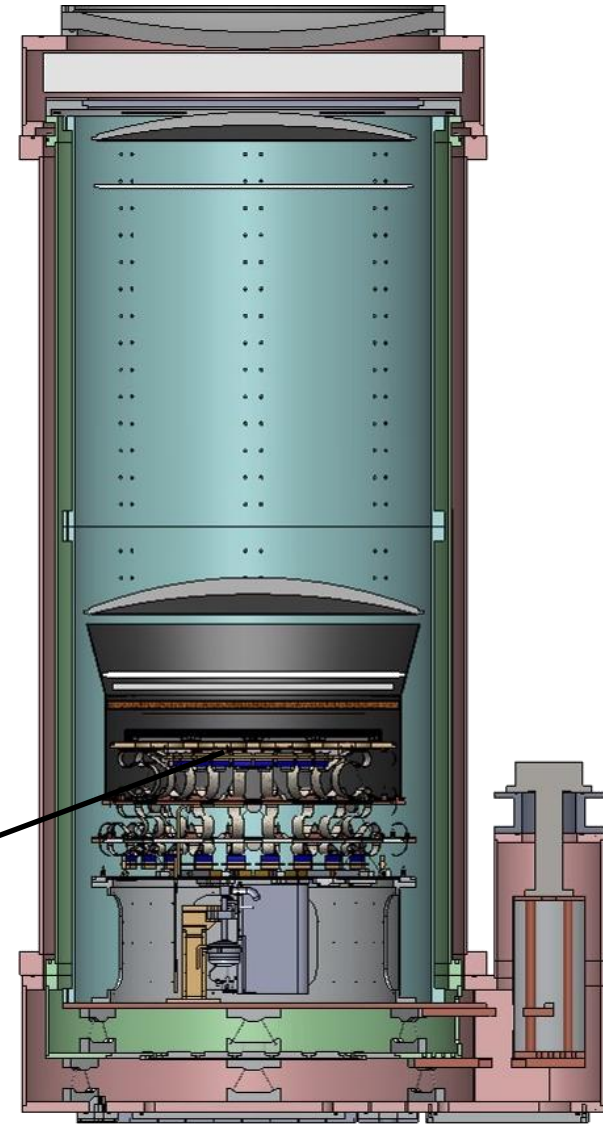
Plug & play detector modules
each have 64 dual-pol 95 GHz
camera pixels and contain cold
multiplexing electronics.

Building BICEP Array



4 wide-field receivers:

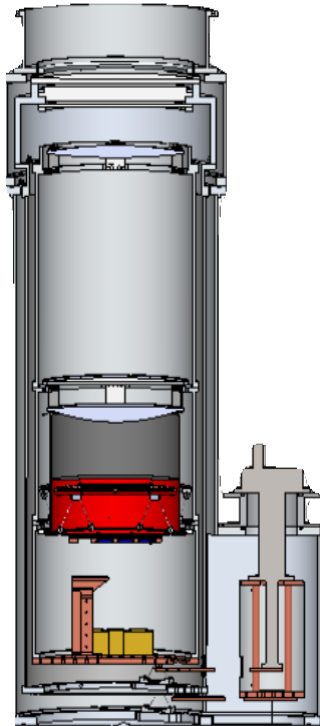
- 30/40 GHz
- 95 GHz
- 150 GHz
- 220/270 GHz



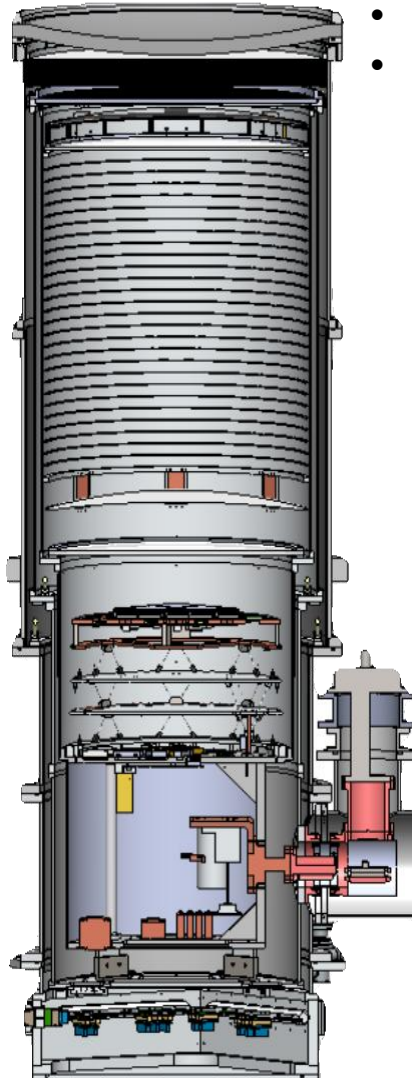
Focal plane layout

BICEP Array vs. predecessors

- 26cm aperture
- 15° FOV
- $f/2.2$ optics

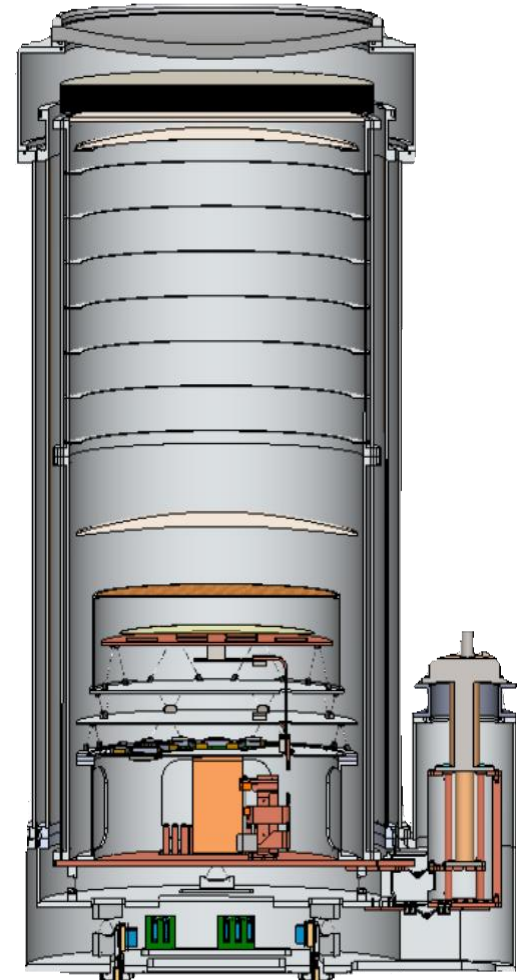


Keck/BICEP2



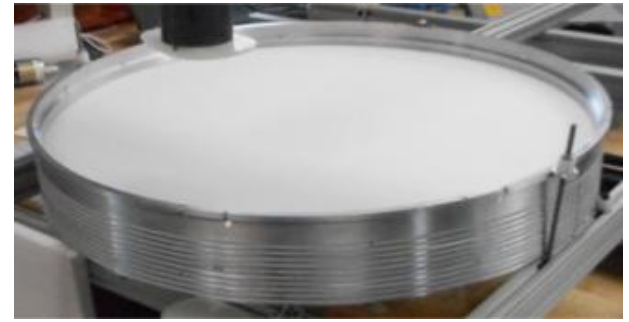
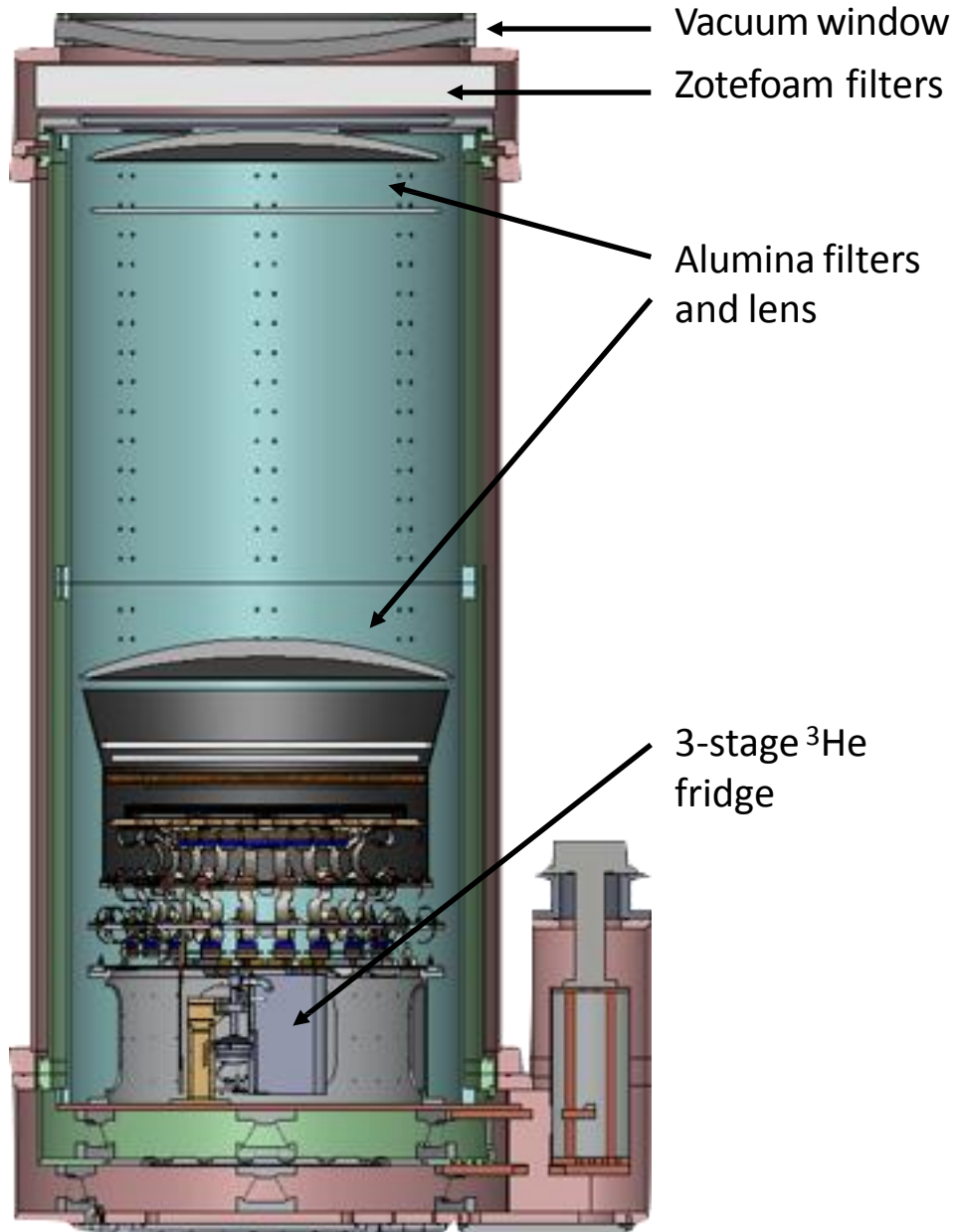
BICEP3

- 52cm aperture
- 28° FOV
- $f/1.7$ optics



BICEP Array

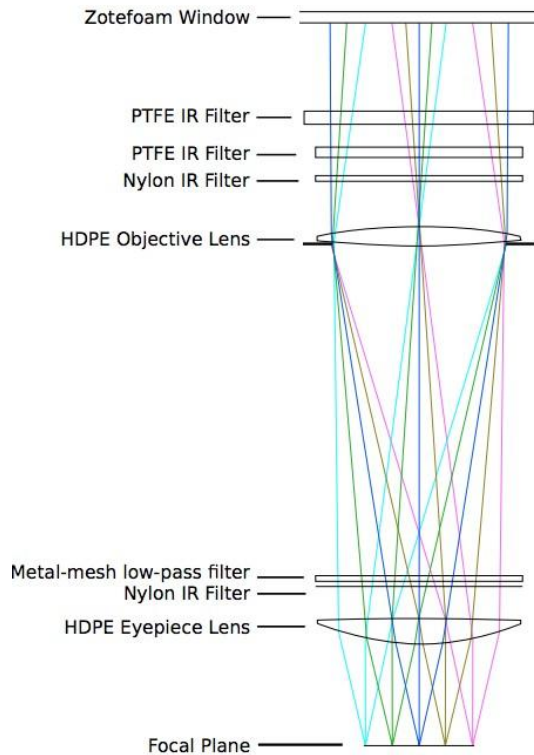
BA receiver



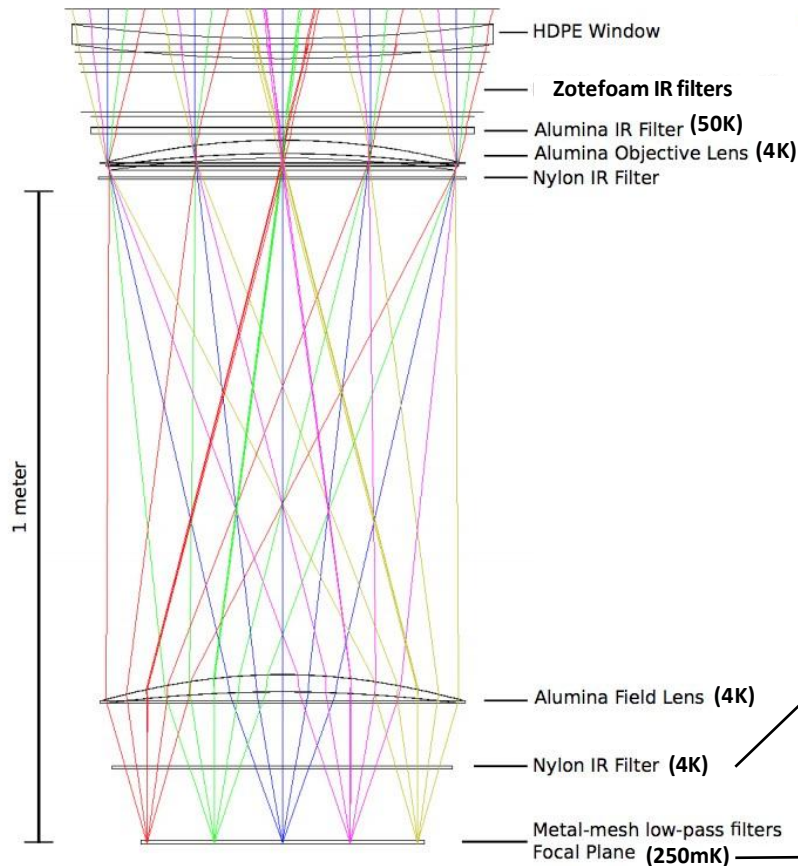
BICEP/Keck Optics

[Only approximately to scale]

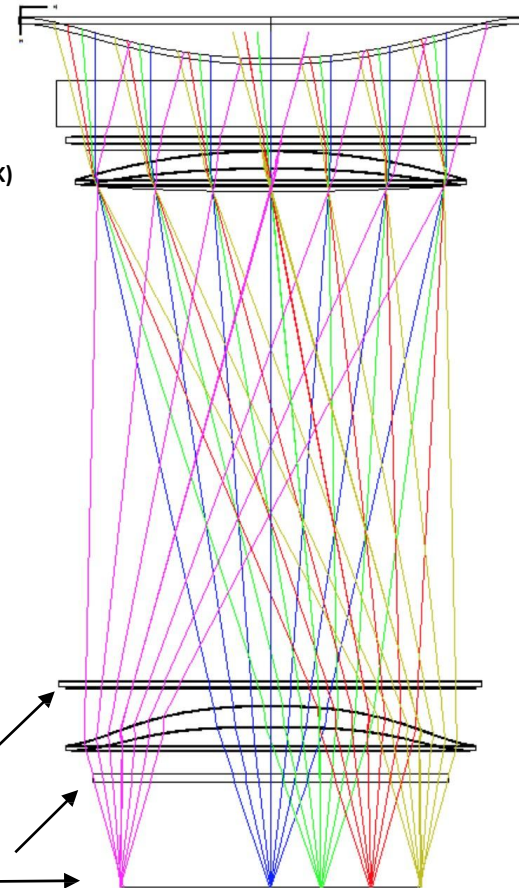
BICEP2/Keck Array



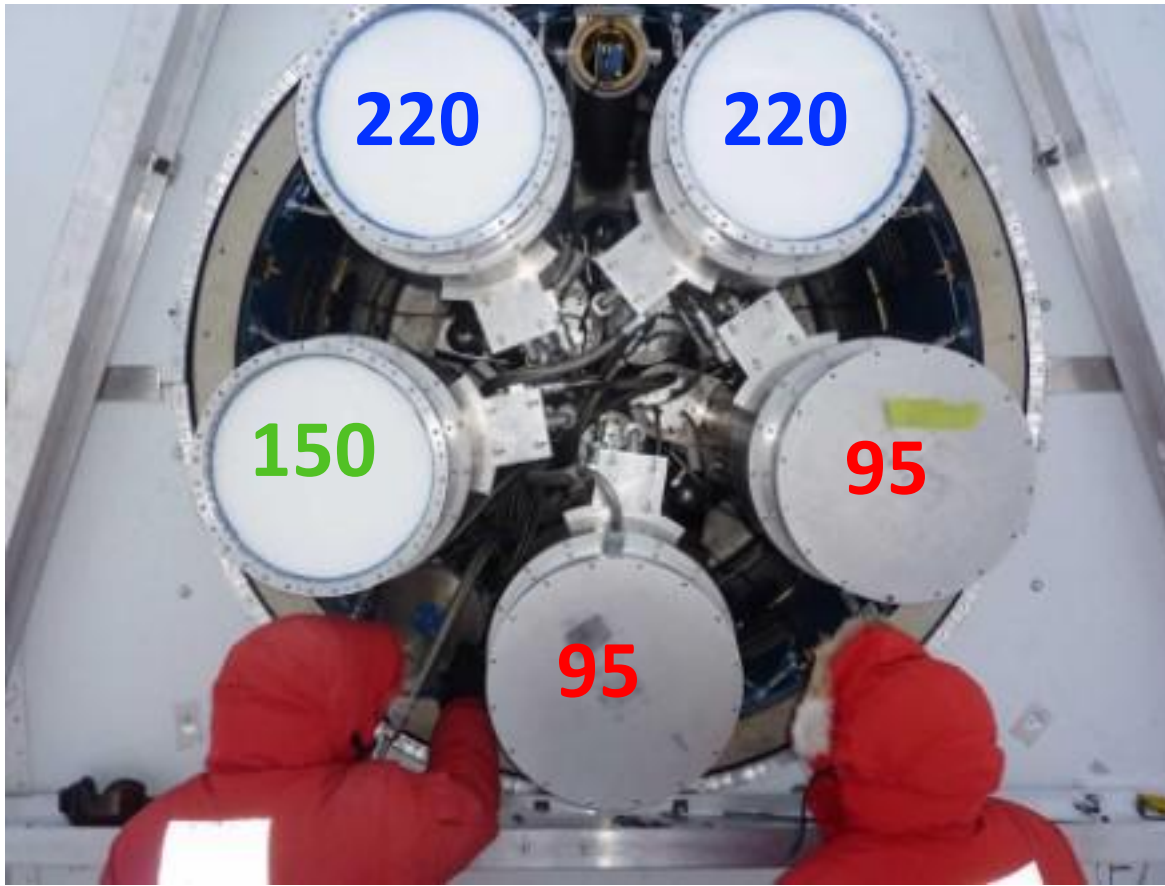
BICEP3



BICEP Array



Keck Array Frequency Coverage

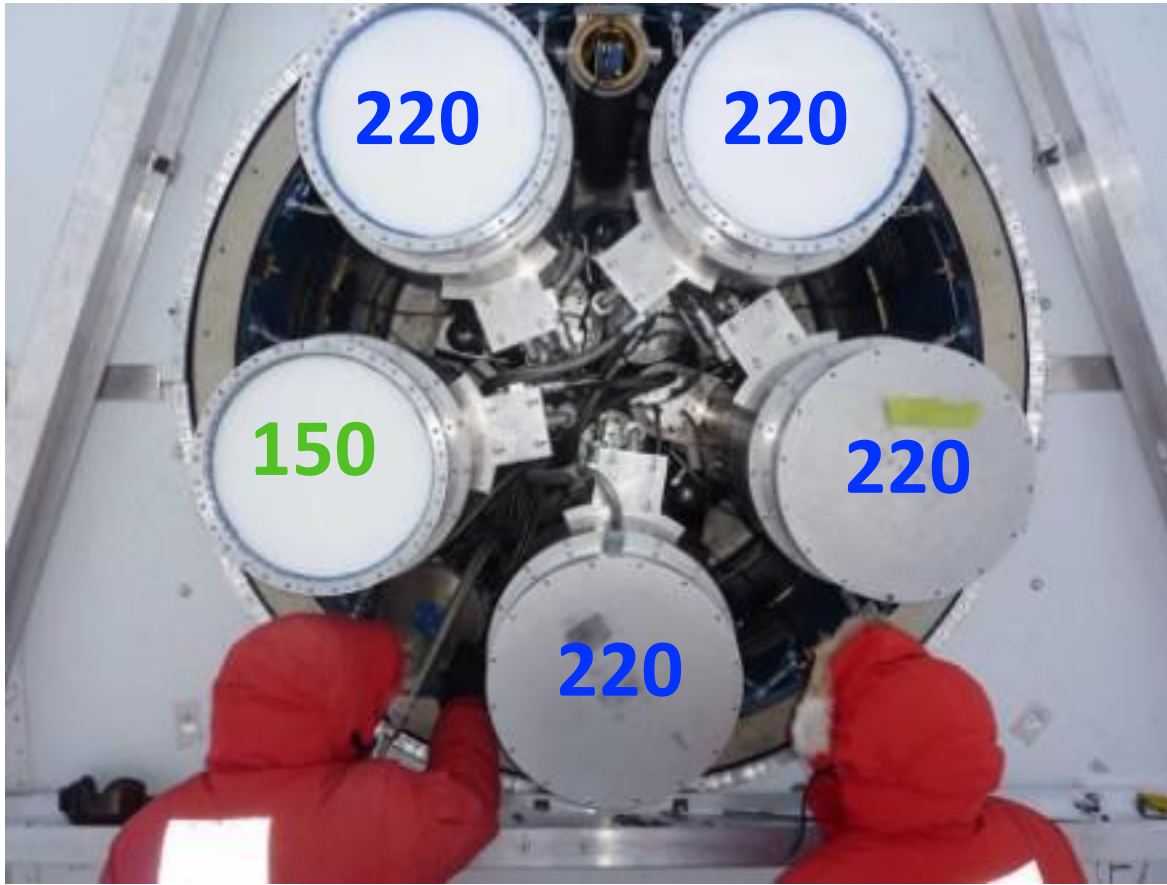


- 2012-2013: All Keck Array receivers at 150 GHz
- 2014: Two 150 GHz receivers replaced with 95 GHz
- 2015: Two additional 150s replaced with 220s

2015

BK15: Out soon!

Keck Array Frequency Coverage

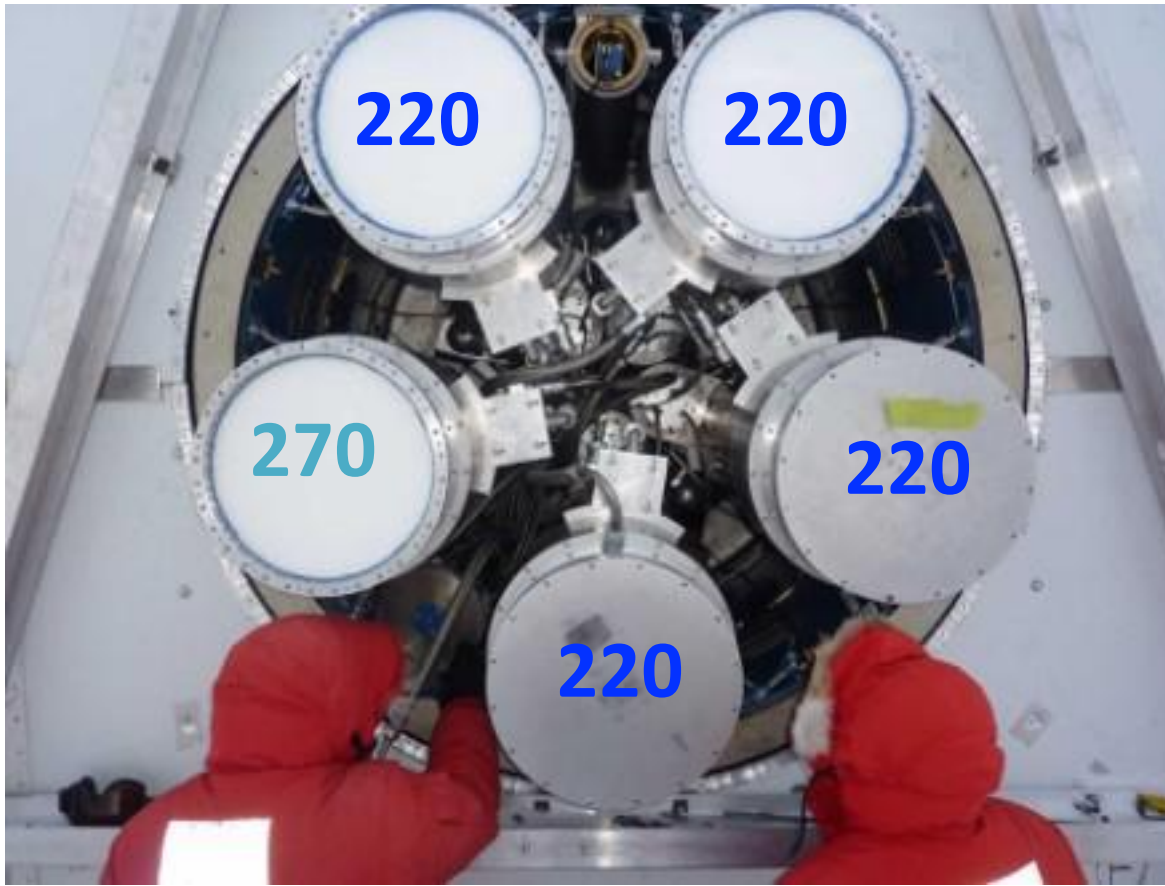


- 2012-2013: All Keck Array receivers at 150 GHz
- 2014: Two 150 GHz receivers replaced with 95 GHz
- 2015: Two additional 150s replaced with 220s
- 2016: Two 95 GHz receivers switched to 220 GHz (BICEP3 now observing at 95 GHz)

2016

Analysis ongoing

Keck Array Frequency Coverage



2017

Analysis ongoing

- 2012-2013: All Keck Array receivers at 150 GHz
- 2014: Two 150 GHz receivers replaced with 95 GHz
- 2015: Two additional 150s replaced with 220s
- 2016: Two 95 GHz receivers switched to 220 GHz (BICEP3 now observing at 95 GHz)
- 2017: Remaining 150 GHz receiver replaced with 270 GHz

Stage 2

Stage 3

BICEP2
(2010-2012)

Keck Array
(2012-2019)

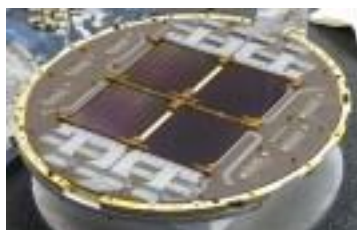
BICEP3
(2015-)

BICEP Array
(2020-)

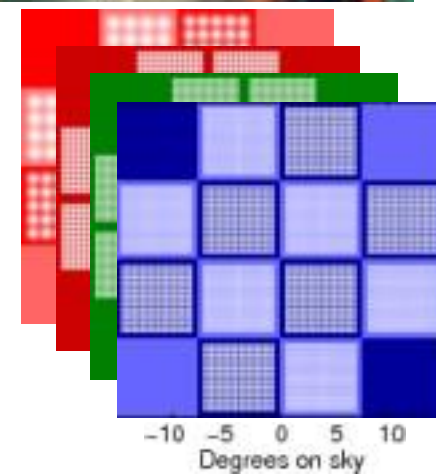
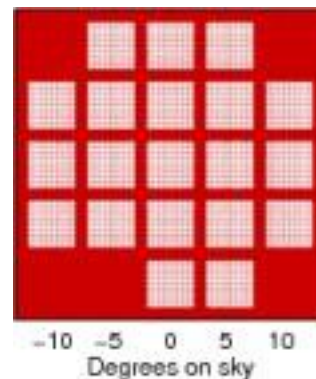
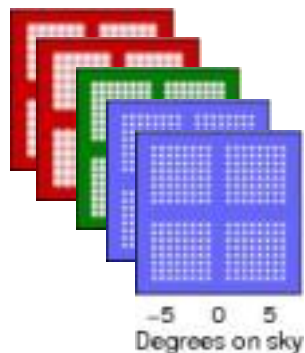
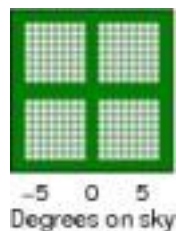
Telescope and Mount



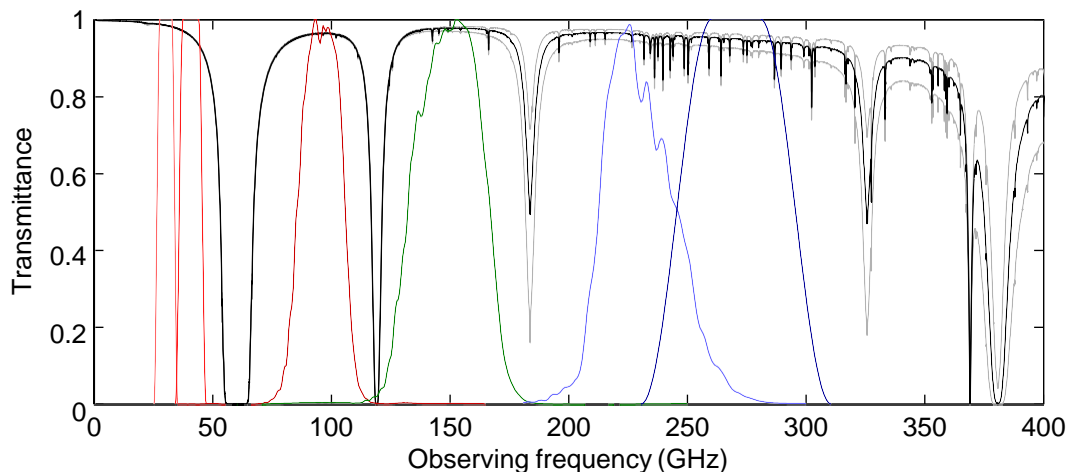
Focal Plane



Beams on Sky



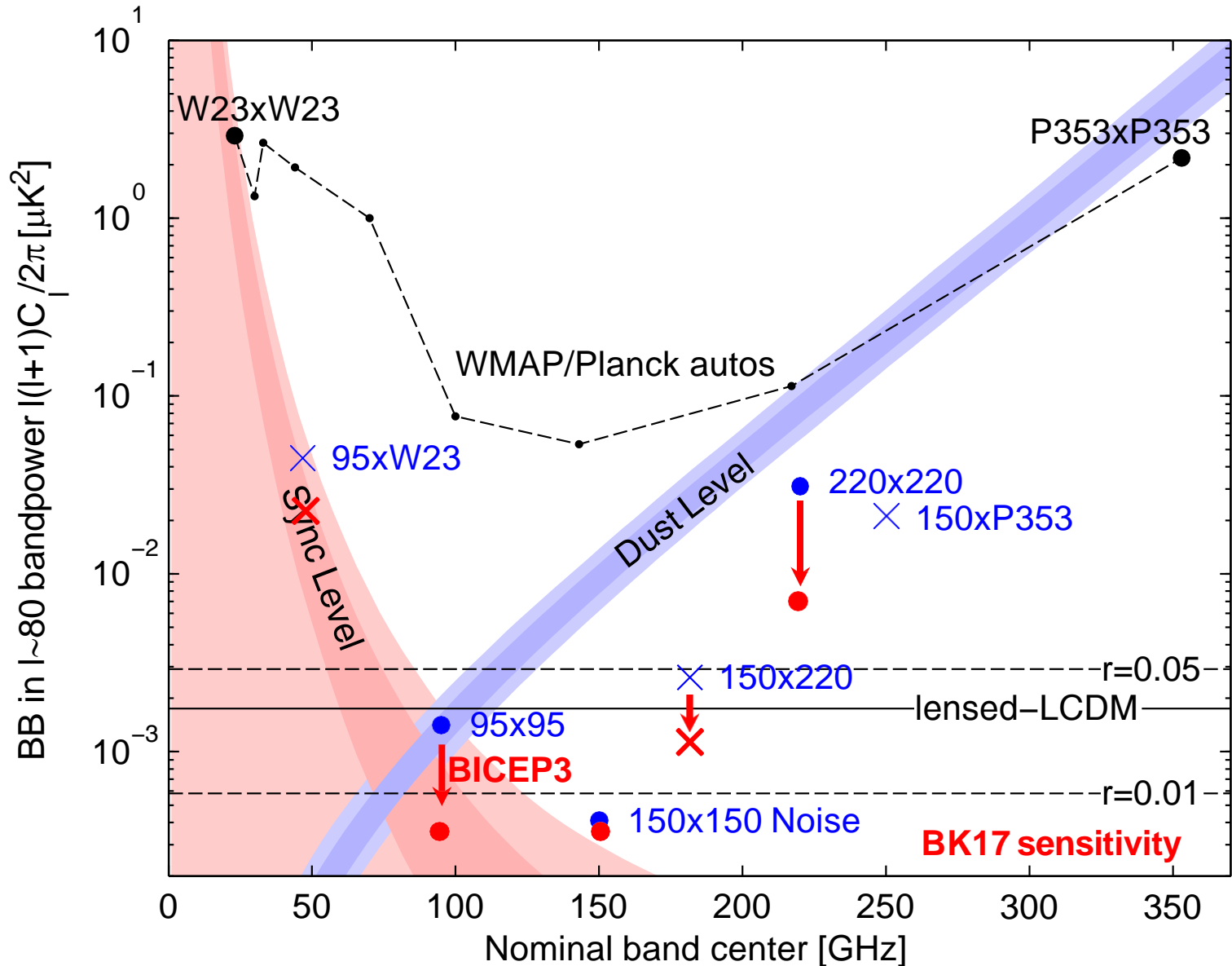
Future BICEP/Keck Frequency Coverage



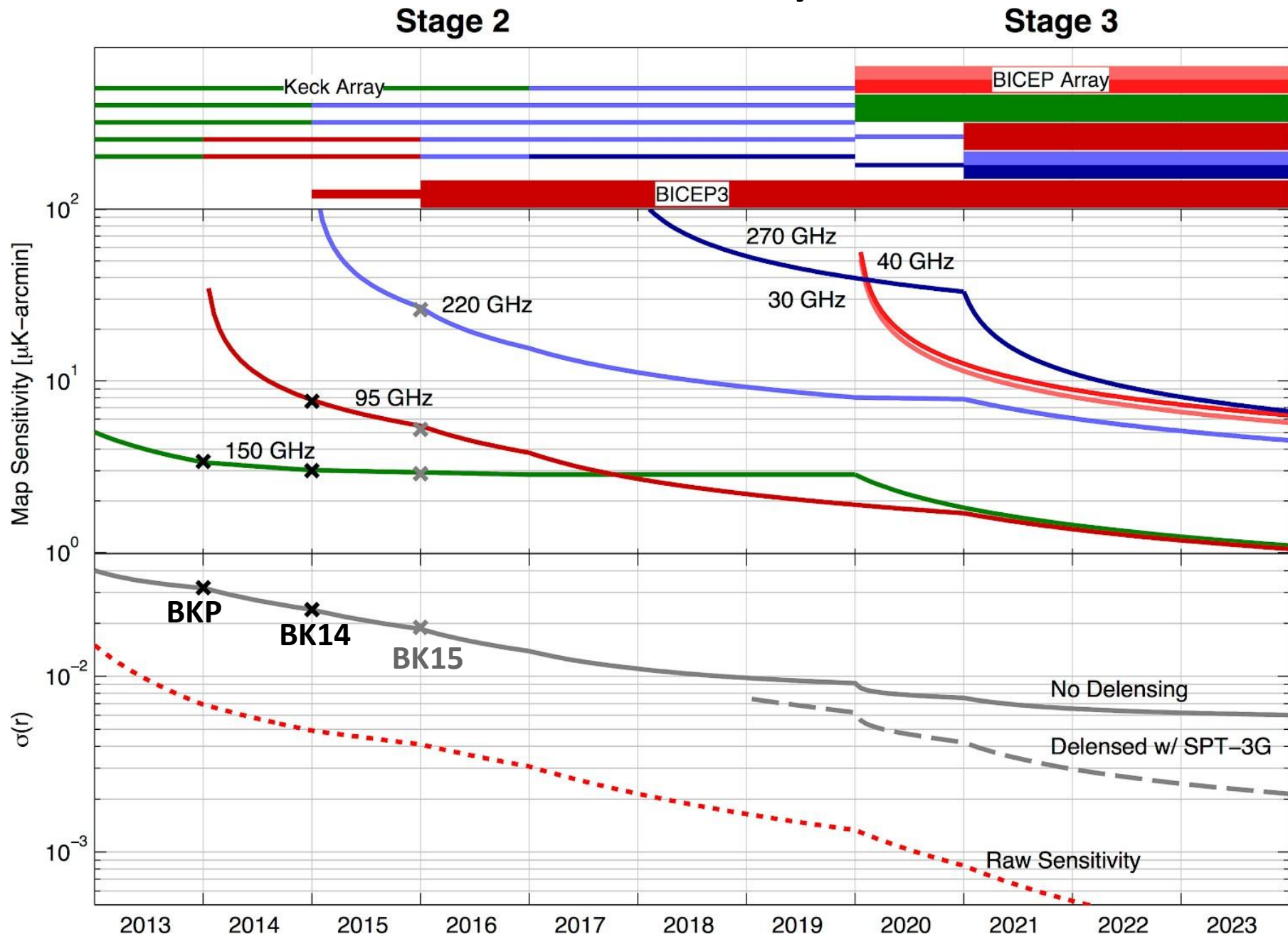
Receiver Observing Band (GHz)	Nominal Number of Detectors	Nominal Single Detector NET ($\mu\text{K}_{\text{CMB}}\sqrt{\text{s}}$)	Beam FWHM (arcmin)	Survey Weight Per Year ($\mu\text{K}_{\text{CMB}}^{-2} \text{yr}^{-1}$)
<i>Keck Array</i>				
95	288	288	43	24,000
150	512	313	30	30,000
220	512	837	21	2,000
270	512	1310	17	800
BICEP3				
95	2560	288	24	213,000
BICEP Array				
< 30	192	221	76	27,000
< 40	300	301	57	21,000
95	3456	288	24	287,000
150	7776	313	15	453,000
< 220	9408	837	11	37,000
< 270	9408	1310	9	15,000

BK15 & BK17 Band Sensitivity (at $l=80$)

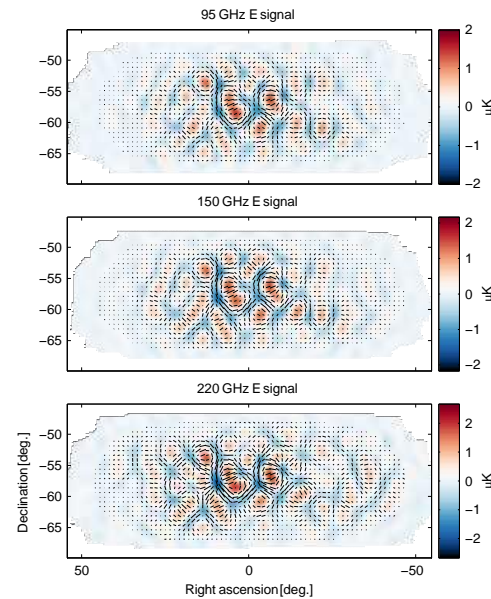
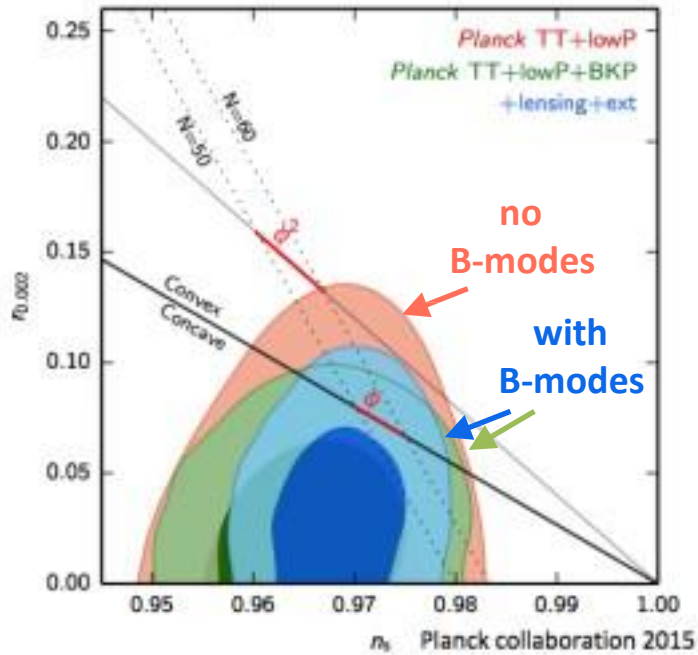
BK17 errors on r will be dominated by synchrotron sensitivity.



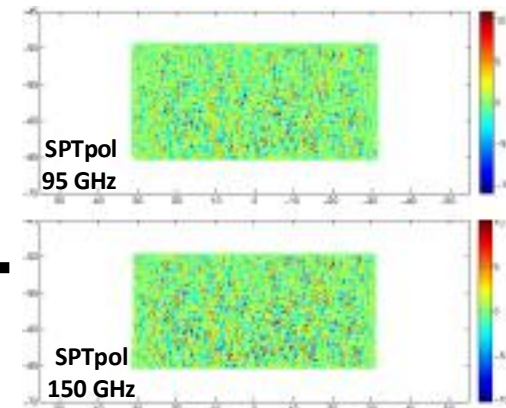
Summary



B-modes now drive progress on r



Deep degree-scale maps:
Multiband for **foreground separation**



Deep high-resolution maps:
Precision delensing

• BICEP-Keck / Planck joint analysis (published Feb 2015):
Raw sensitivity with no foregrounds or lensing: $\sigma(r) = 0.006$
It is now all about component separation!

→ $\sigma(r) = 0.034$ (arXiv:1502.00612)

• 2014 BICEP/Keck analysis adds deep 95 GHz

→ $\sigma(r) = 0.025$ (arXiv:1510.09217)

• 2015 BICEP/Keck analysis adds deep 220 GHz

→ Expect $\sigma(r) = 0.019$ (June 2018)

• 2017 BICEP/Keck + SPTpol delensing

→ Expect $\sigma(r) = 0.010$ (Analysis ongoing)

• 2020-2022+ BICEP Array + SPT3G

→ Forecast $\sigma(r) \sim 0.003$

Conclusions

- BICEP/Keck lead the field in the quest to detect or set limits on inflationary gravitational waves:
 - Best published sensitivity to date
 - Best proven systematic control at degree angular scales
- BK14: Adding 2014 data including, for the first time, at 95GHz:
 - Modest improvement: $r_{0.05} < 0.12$ goes to $r_{0.05} < 0.09$
 - Important milestone: for the first time B-mode only constraint exceeds the sensitivity of TT-derived constraint ($r_{0.05} < 0.12$)
- BK15: Adding 2015 data, which includes 220GHz:
 - Expected $\sigma(r) = 0.019$
 - Now able to explore more data/model variations
- And we can go much further:
 - BICEP3 is online at 95 GHz
 - Delensing using SPT/SPT-3G
 - BICEP Array – $\sigma(r) = 0.003$